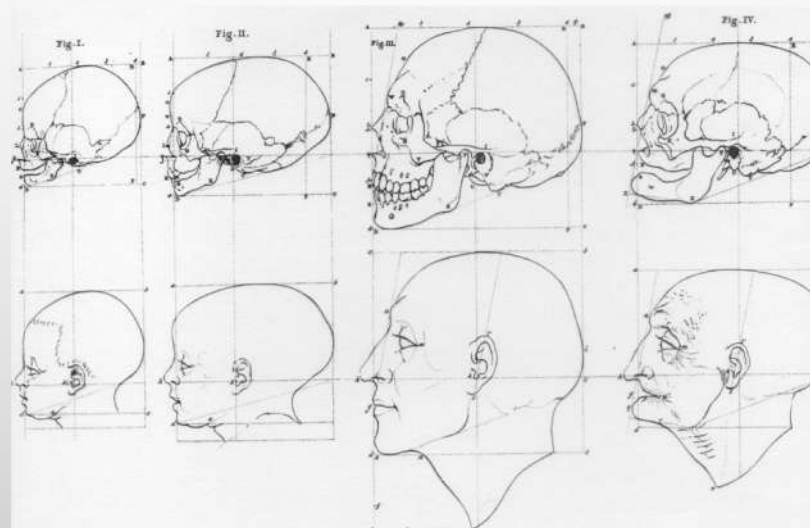


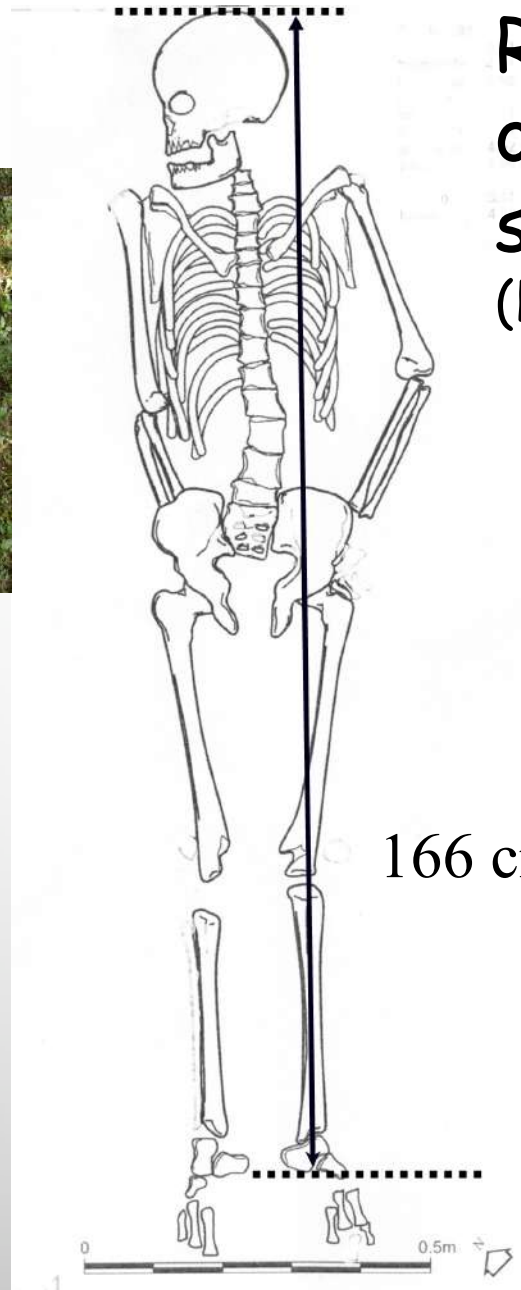
BIOLOGIA DELLO SCHELETRO UMANO

Lezione 4



OTTO DOMANDE PER L'ANTROPOLOGO:

- 1. è un osso umano?*
- 2. è un reperto recente?*
- 3. sono presenti più persone?*
- 4. di quale origine etnica?*
- 5. di che sesso?*
- 6. di che età ?*
- 7. di quale statura?*
- 8. con quali caratteristiche?*



Rilevazione *in situ*,
o dal disegno in
scala
(Hanson 1992)



Determinazione della statura in laboratorio

La misura della statura può essere determinata dallo scheletro **sommando tutte le lunghezze delle ossa** che concorrono a determinarla e **stimando lo spessore delle cartilagini**.



Individuo 386C, Necropoli di Spina (VI-III sec.). Foto: A. Vecchi



Dalla misura delle ossa, a seconda del sesso, età e della popolazione, si può det. la statura usando delle **formule** . Anche in questo caso **si ottiene un intervallo**, più che un singolo valore.

Equations Used to Estimate Stature, in Centimeters, with Standard Error, from the Long Bones of Various Groups of Individuals between 18 and 30 Years of Age^a

**TROTTER,
1970**

Si utilizzano le lungh. mx (meglio fare una media da diverse ossa)



White Males			Black Males		
3.08	Hum + 70.45	± 4.05	3.26	Hum + 62.10	± 4.43
3.78	Rad + 79.01	± 4.32	3.42	Rad + 81.56	± 4.30
3.70	Uln + 74.05	± 4.32	3.26	Uln + 79.29	± 4.42
2.38	Fem + 61.41	± 3.27	2.11	Fem + 70.35	± 3.94
2.68	Fib + 71.78	± 3.29	2.19	Fib + 85.65	± 4.08
White Females			Black Females		
3.36	Hum + 57.97	± 4.45	3.08	Hum + 64.67	± 4.25
4.74	Rad + 54.93	± 4.24	2.75	Rad + 94.51	± 5.05
4.27	Uln + 57.76	± 4.30	3.31	Uln + 75.38	± 4.83
2.47	Fem + 54.10	± 3.72	2.28	Fem + 59.76	± 3.41
2.93	Fib + 59.61	± 3.57	2.49	Fib + 70.90	± 3.80
East Asian Males			Mexican Males		
2.68	Hum + 83.19	± 4.25	2.92	Hum + 73.94	± 4.24
3.54	Rad + 82	± 4.60	3.55	Rad + 80.71	± 4.04
3.48	Uln + 77.45	± 4.66	3.56	Uln + 74.56	± 4.05
2.15	Fem + 72.57	± 3.80	2.44	Fem + 58.67	± 2.99
2.40	Fib + 80.56	± 3.24	2.50	Fib + 75.44	± 3.52

^aTo estimate stature of older individuals, subtract 0.06 (age in years, 30) cm; to estimate cadaver stature, add 2.5 cm. From Trotter (1970). The tibia is not included; see text for rationale.

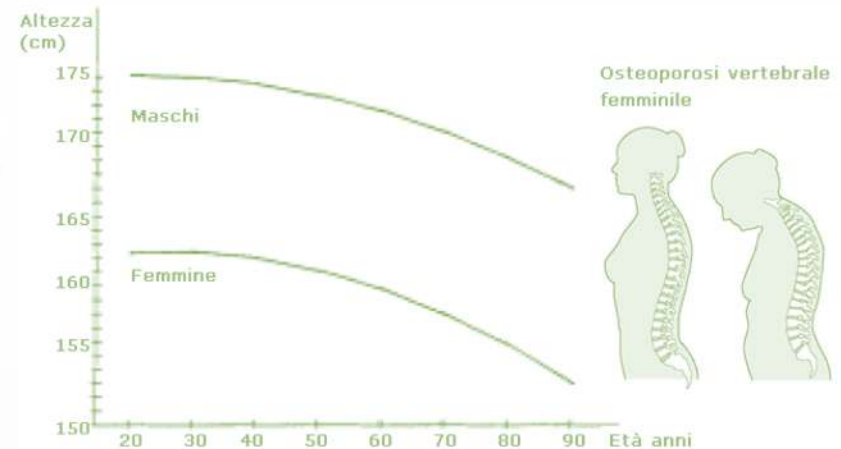
Es.: Qual'era la statura di un individuo M caucasioide, se il suo femore era lungo 45.0 cm?

$2.38 \times 45.0 + 61.41 = 168.51 \pm 3.27 \text{ cm}$

165.2 - 171.8 cm

EFFETTO dell'INVECCHIAMENTO SULLA STATURA

Trotter e Gleser consigliavano semplicemente di ridurre il valore di statura stimato di **0.06 mm** per ogni anno di età sup.ai 30 anni (in base a studi trasversali)



(studi longitudinali)

Table 4

AMOUNT IN MILLIMETERS THAT SHOULD BE SUBTRACTED FROM TROTTER AND GLESER STATURE ESTIMATIONS TO COMPENSATE FOR AGING IN SUBJECTS OVER AGE 45

Age	Males	Females
50	4.3	0.4
55	7.4	2.8
60	11.5	7.0
65	16.4	12.9
70	22.2	20.2
75	28.6	28.8
80	35.6	38.5
85	43.2	49.0

Tavole di Manouvrier (1892)

Fibula mm	Tibia mm	Femore mm	Statura cm	Omero mm	Radio mm	Ulna mm
MASCHI						
318	319	392	153,0	295	213	227
323	324	398	155,2	298	216	231
328	330	404	157,1	302	219	235
333	335	410	159,0	306	222	239
338	340	416	160,5	309	225	243
344	346	422	162,5	313	229	246
349	351	428	163,4	316	232	249
353	357	434	164,4	320	236	253
358	362	440	165,4	324	239	257
363	368	446	166,6	328	243	260
368	373	453	167,7	332	246	263
373	378	460	168,6	336	249	266
378	383	467	169,7	340	252	270
383	389	475	171,6	344	255	273
388	394	482	173,0	348	258	276
393	400	490	175,4	352	261	280
398	405	497	176,7	356	264	283
403	410	504	178,5	360	267	287
408	415	512	181,2	364	270	290
413	420	599	183,0	368	273	293

M

Più usate in Eu. Sottostimano stat. M, sovrastimano stat. F.
Manca intervallo.

Es.: Qual'era la statura di un individuo M caucasoide, se il suo femore era lungo 45.0 cm?

MANOUVRIER, 1892

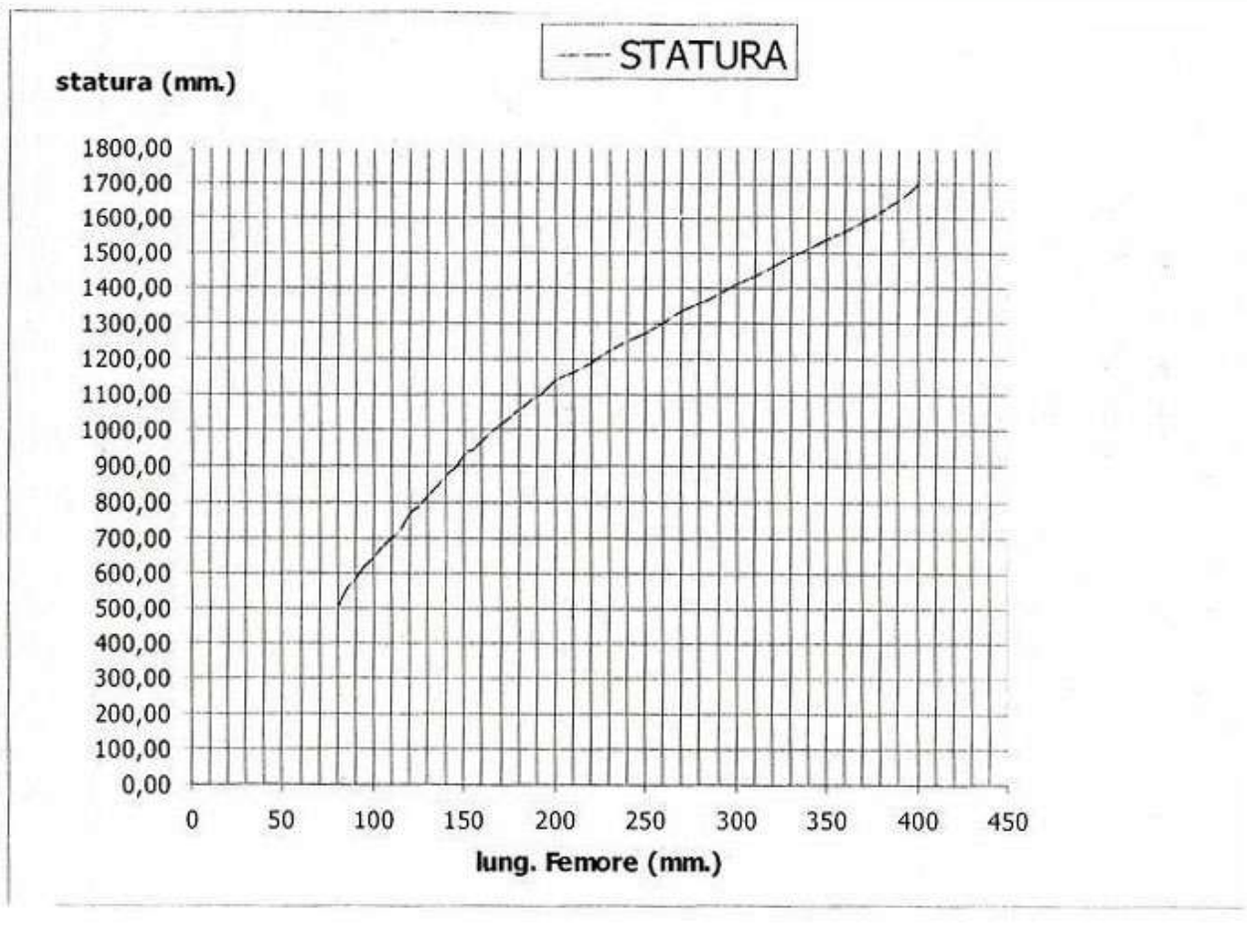
F

Fibula mm	Tibia mm	Femore mm	Statura cm	Omero mm	Radio mm	Ulna mm
288	289	368	142,0	266	195	206
293	294	373	144,0	270	197	209
298	299	378	145,5	273	199	212
303	304	383	147,0	276	201	215
307	309	388	148,8	279	203	217
311	314	393	149,7	282	205	219
316	319	398	151,3	285	207	222
320	324	403	152,8	289	209	225
325	329	408	154,3	292	211	228
330	334	415	155,6	297	214	231
336	340	422	156,8	302	218	235
341	346	429	158,2	307	222	239
346	351	436	159,5	313	226	243
351	358	443	161,2	318	230	247
356	364	450	163,0	324	234	251
361	370	457	168,0	329	238	254
366	376	464	167,0	334	242	258
371	382	471	169,2	339	246	261
376	388	478	171,5	344	250	264

*Per omero, radio, ulna: lungh.mx.
Femore: lungh.fisiol.
Tibia: lungh.tot.(senza spina)*

Si basa sui dati che il Rollet (1888) aveva rilevato su **100 cadaveri** dell'ospedale di Lione, per ognuno dei quali era stata misurata la statura e la lunghezza delle ossa lunghe degli arti.

Calcolo statura in individui giovani



Calcolo lunghezza del feto

Metodo Balthazard e Derivieux (1921)

$$S = 5,6 \times \text{lunghezza della diafisi femorale} + 8 \text{ cm.}$$

$$S = 6,5 \times \text{lunghezza della diafisi omerale} + 8 \text{ cm.}$$

$$S = 6,5 \times \text{lunghezza della diafisi della tibia} + 8 \text{ cm.}$$

Metodo Olivier e Pineau (1958)

$$S = 7,92 \times \text{lunghezza della diafisi omerale} - 0,32 \pm 1,8 \text{ cm.}$$

$$S = 8,73 \times \text{lunghezza della diafisi dell'ulna} - 1,07 \pm 1,59 \text{ cm.}$$

$$S = 6,29 \times \text{lunghezza della diafisi del femore} + 4,42 \pm 1,82 \text{ cm.}$$

$$S = 7,85 \times \text{lunghezza della diafisi della fibula} + 2,78 \pm 1,55 \text{ cm.}$$

$$S = 7,39 \times \text{lunghezza della diafisi della tibia} + 3,55 \pm 1,8 \text{ cm}$$

S= lunghezza corpo

LUNGH. FETALE	ETA' IN MESI LUNARI	LUNGH. FETALE	ETA' IN MESI LUNARI
17,65	4 ¼	37,85	7 ¼
19,81	4 ½	39,13	7 ½
21,88	4 ¾	40,37	7 ¾
23,80	5	41,58	8
25,64	5 ¼	42,74	8 ¼
27,40	5 ½	43,84	8 ½
29,08	5 ¾	44,97	8 ¾
30,69	6	46,03	9
32,23	6 ¼	47,07	9 ¼
33,72	6 ½	48,08	9 ½
35,15	6 ¾	49,06	9 ¾
36,52	7	50,02	10 NASCITA

Stima
dell'Età
del
feto da
S

Oppure: $ETA' = 5,6 \times \text{lunghezza fetale.}$

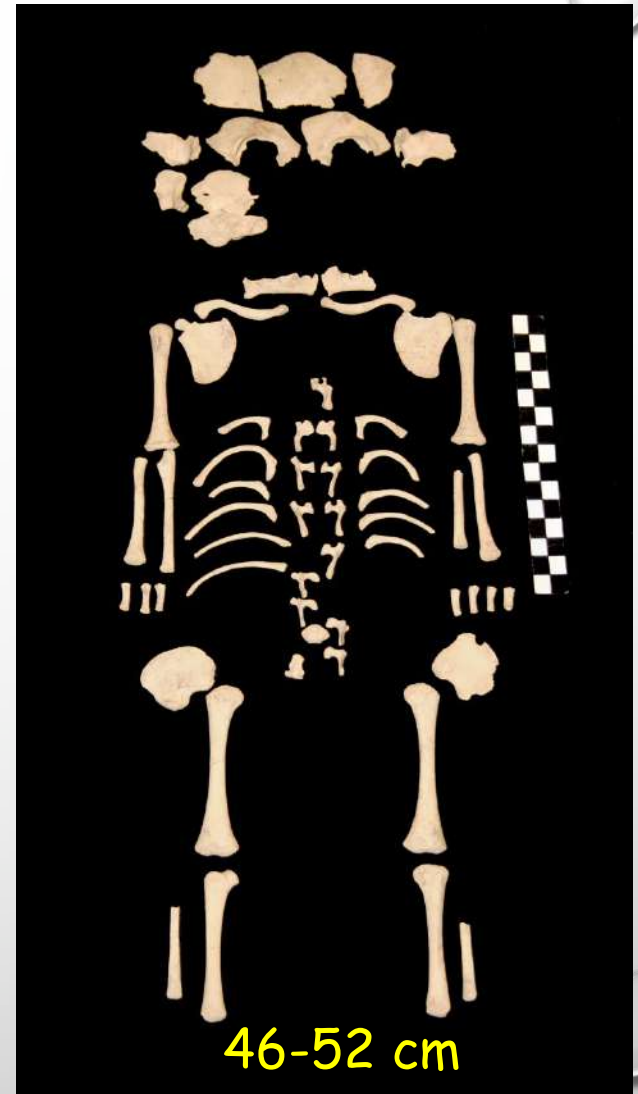
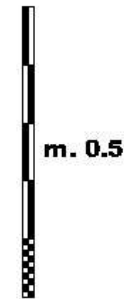
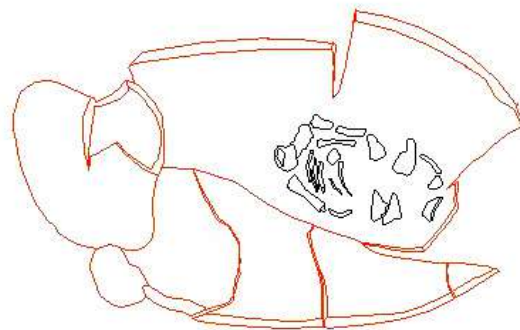
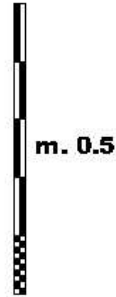
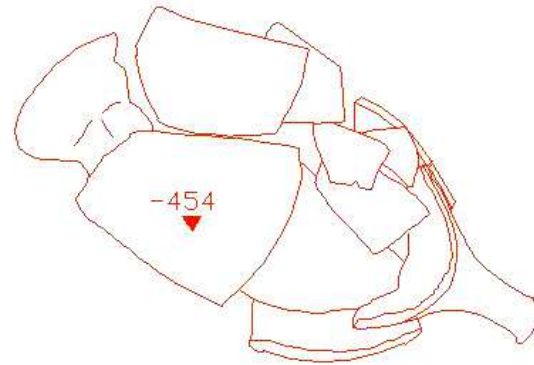
Esempio: se la lungh. Calcolata (S) è 24 cm
Età = $5.6 \times 24 = 134.4$ gg

Mese lunare = 27 giorni 7 ore 43 minuti

4.98 mesi lunari

necropoli di epoca romana

Tb 110



9.2 mesi lunari

Con il metodo di Olivier e Pineau



UNIVERSITÀ
DEGLI STUDI
DI FERRARA
- EX LABORE FRUCTUS -



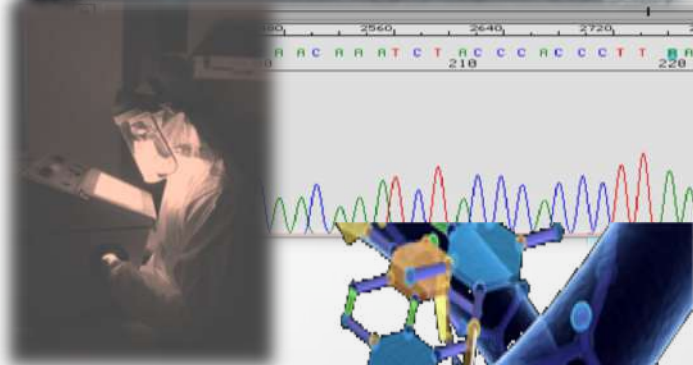
European Research Council
Established by
the European Commission

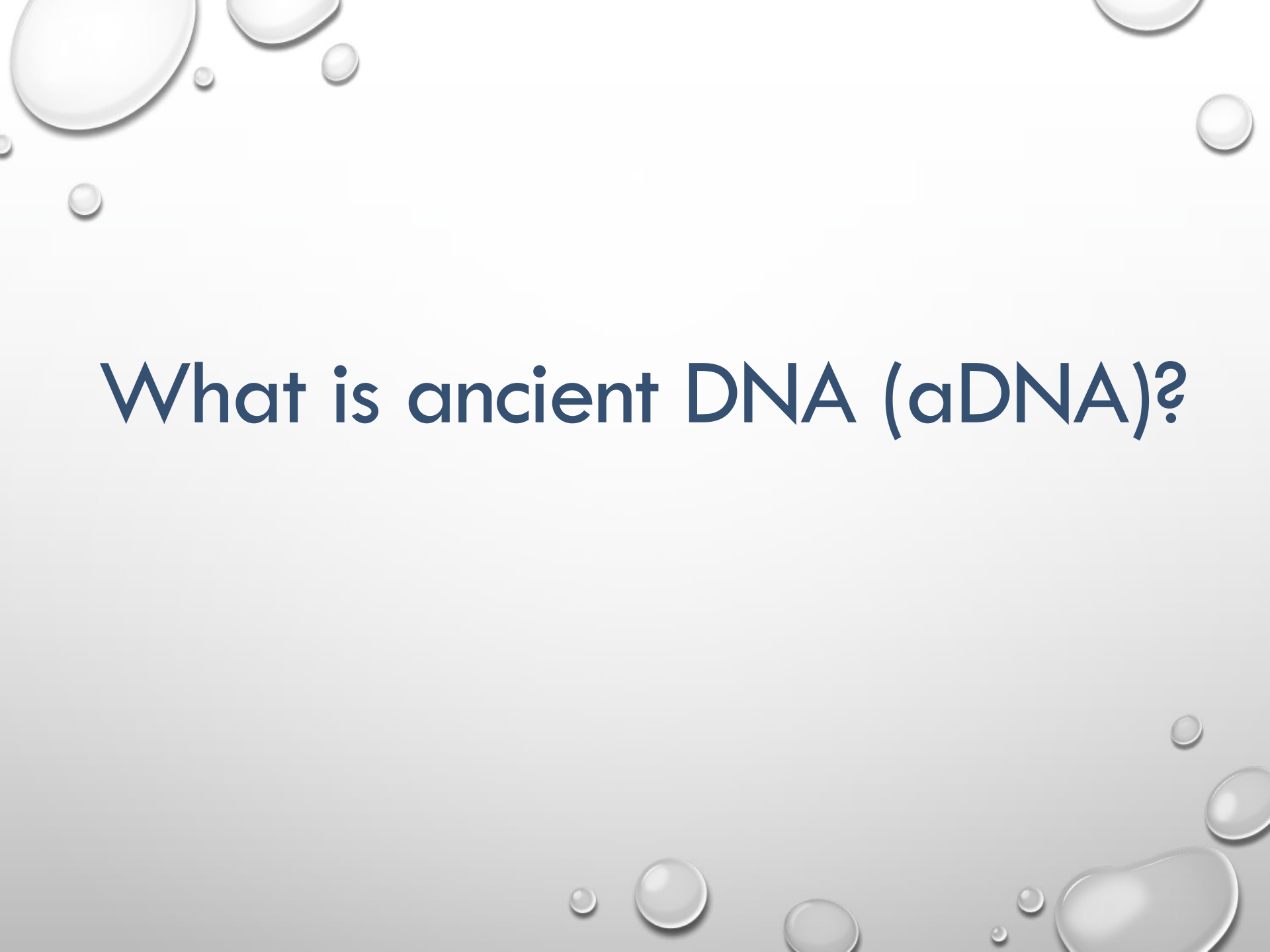
CEES

Centre for Ecological and Evolutionary Synthesis

Ancient DNA (aDNA) Analyses of Human remains: 36 years of evolution of a scientific discipline

Barbara Bramanti





What is ancient DNA (aDNA)?



**Human
Body**

CELLS



TISSUES



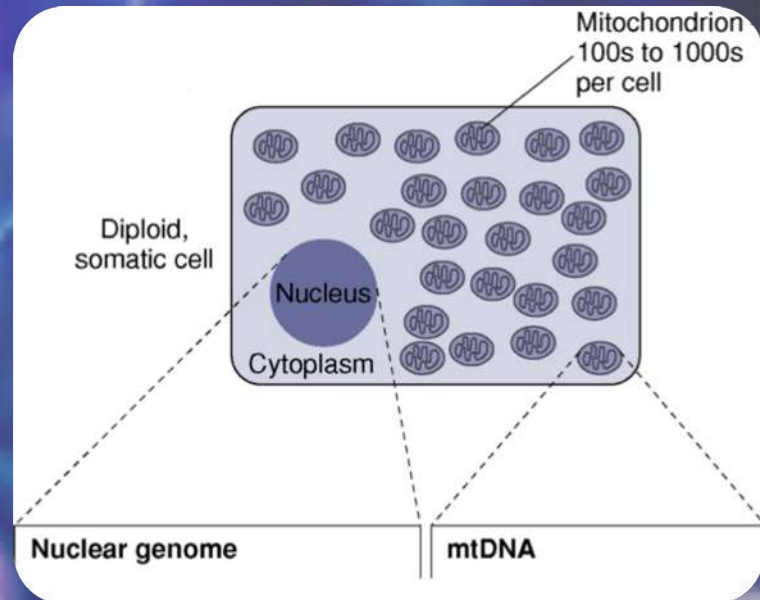
ORGANS



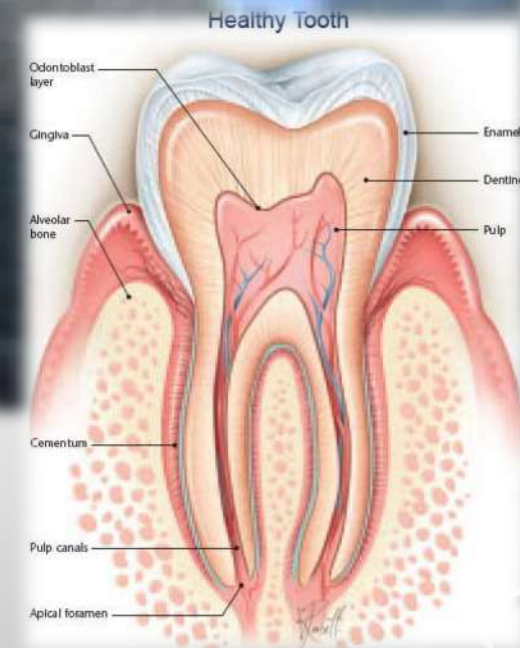
SYSTEMS



3DSCIENCE.COM
MeridianLife
Vitamins, Fats, Acids, Minerals



Human hard Tissues (Bones and Teeth)



Petrous part of temporal bone (Pars petrosa; Pinhasi et al. 2015)

Other sources of aDNA



Corpi imbalsamati



Mummie naturali



Capelli



Tartaro



Preparati anatomici



A



Insetti



Artefatti



Sedimenti



Coproliti



Piante, frutti

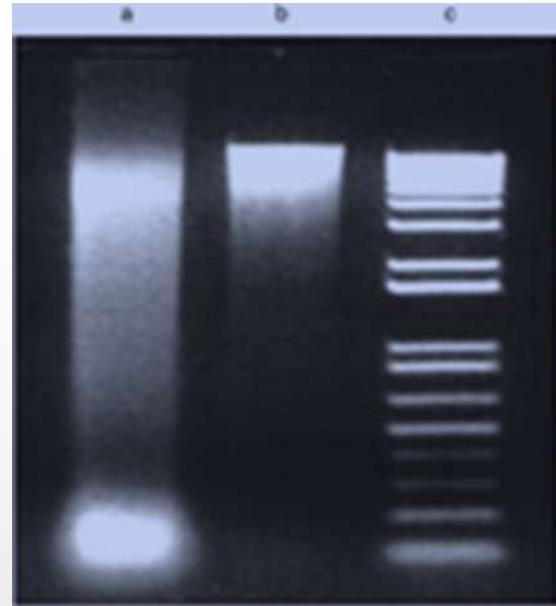


Chewing-gum
(di 5000 anni fa)

- DNA umano
- DNA animale
- DNA vegetale
- DNA batterico
- DNA fungino
- ...

Ancient DNA (aDNA)

- Degraded, demaged fragmented DNA
- Low amount
- *Postmortem* base modifications
- Prone to environmental contamination



aDNA

Modern DNA



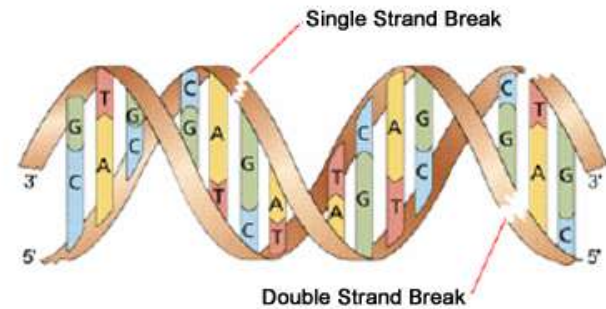
Alignment of fragmented DNA



Comparison with other (modern & ancient) genomes

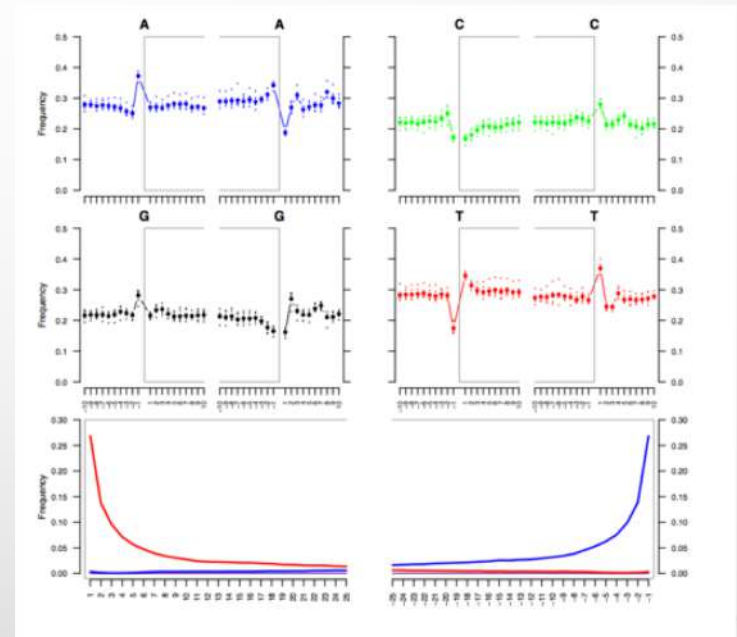
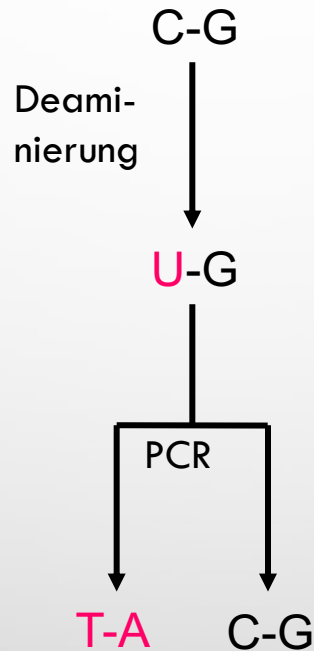
Typical aDNA damages:

BREAKS are due to Oxidative lesions



SOME NUCLEOTIDES ARE DIFFERENT FROM THE ORIGINAL ONES

Hydrolytic lesions (water)



How long can aDNA survey?

Ideal environments!

Types of decay inducing environments:

- Presence of moisture
- High temperatures
- Presence of Micro-Organisms, insect, fungi
- Acidity (-pH)



2014: mitochondrial genome of a hominin that lived more than 400,000 years ago; Exomes from two Neanderthal individuals (more than 40,000 YBP); nearly complete nuclear genome from a 45,000-year-old modern human fossil.

2016: 430,000-year-old DNA of a pre-Neanderthal found in Spain's Sima de los Huesos.

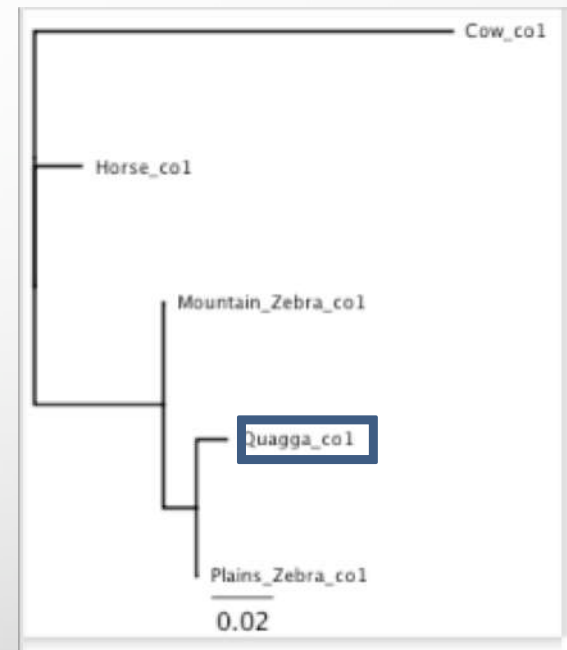
2013: full genome of an ancestral horse species (permafrost of North America more than 700,000 years ago) - the oldest complete genome sequenced thus far.⁴

The background features a light gray gradient with several realistic water droplets of various sizes scattered in the corners. The droplets have highlights and shadows, giving them a three-dimensional appearance. The text is centered in the middle of the page.

A bit of History...

1984 Russell G. Higuchi and colleagues carried out the first complete ancient DNA study

Higuchi R, Bowman B, Freiberger M, Ryder OA, Wilson AC, *DNA sequences from the quagga, an extinct member of the horse family*, in *Nature*, vol. 312, n° 5991, 1984, pp. 282–4



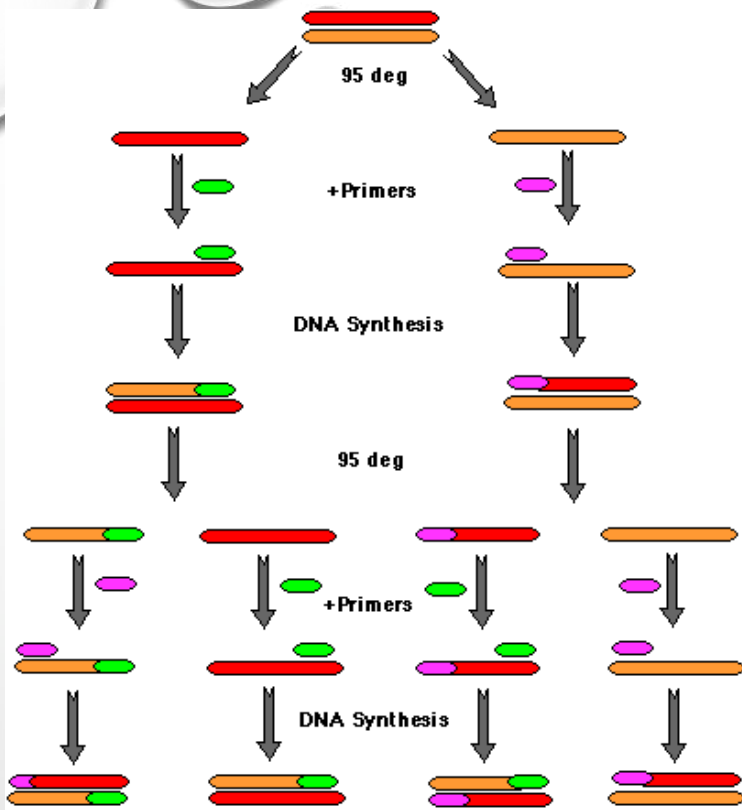
Family of quaggas (*Equus quagga quagga*), 150 years old, at the Naturhistorische Museum in Mainz

Pääbo, S. Molecular cloning of Ancient Egyptian mummy DNA, *Nature* **314**, 644-645 (1985)

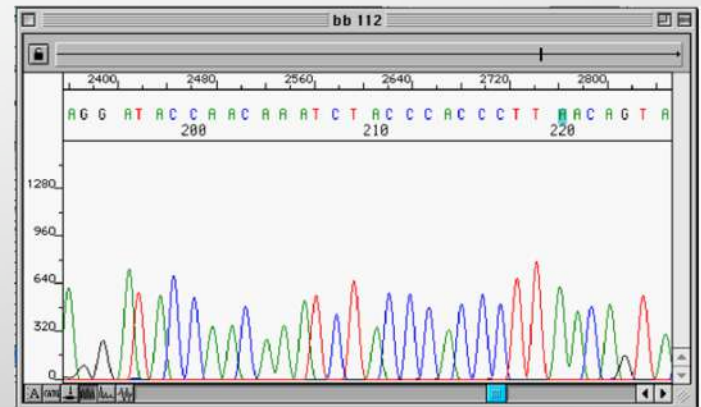


The first ancient human sequence (ca. 2,400 YBP) contained only two sequencing errors (1989).





1984 K. Mullis
invented the PCR

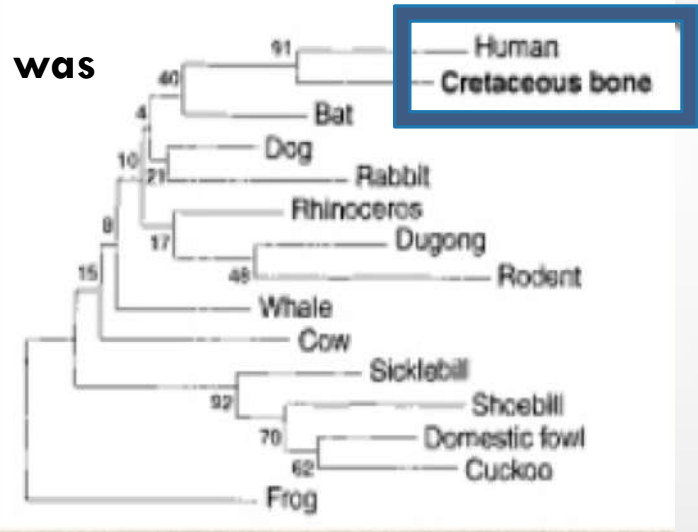


1994. Scott Woodward claimed to have sequenced
aDNA from an 80 million years old Dinosaur bone



CANO, R. J., H. N. POINAR, D. W. ROUBIK, and G. O. POINAR JR. 1992. Enzymatic amplification and nucleotide sequencing of portions of the 18s rRNA gene of the bee *Proplebeia dominicana* (Apidae: Hymenoptera) isolated from 25-40 million year old Dominican amber. *Med. Sci. Res.* 20:619- 622.

1995. S.B. Hedges, S. Paabo and M. Allard demonstrated that **Woodward's dinosaur DNA was instead (male) human DNA**



Poly professor brews beer with 45-million-year-old yeast (January, 18th, 2011)



Continuing concerns about the rigor of research on ancient DNA and that "high-profile journals continue to publish studies that do not meet the necessary controls" prompt a list summarizing "criteria of authenticity" required for work published in this area. The role of the polio vaccination program carried out in Central Africa in the late 1950s in the origin of HIV and AIDS (as posited in the book *The River*) is hotly debated. And "the myth...that efficient use of nuclear resources is a proliferation threat" is challenged, and it is suggested that "electricity produced from existing nuclear by-products would be equivalent to that needed by the United States, at present use rates, for hundreds of years."

Ancient DNA: Do It Right or Not at All

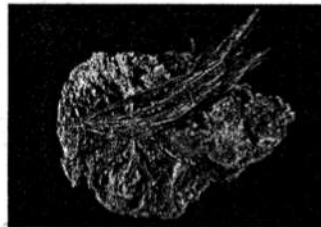
At the recent 5th International Ancient DNA Conference in Manchester, U.K., reported by Erik Stokstad in his News Focus article "Divining diet and disease from DNA" (28 Jul., p. 530), one presentation boldly opened with the claim that the field was now mature and could move ahead with confidence. This optimism is unfounded, as demonstrated by the notable absence of "criteria of authenticity" from many presentations at the conference. Ancient DNA research presents extreme technical difficulties because of the minute amounts and degraded nature of surviving DNA and the exceptional risk of contamination. The need to authenticate results became obvious in the mid-1990s when a series of high-profile studies were shown to be unrepeatable (1). For example, DNA reputed to come from a dinosaur (2) was actually contamination by a human mitochondrial gene insertion in the nucleus (numt) (3). Over the ensuing years, criteria have been developed and put into practice by some practitioners in the field. Regrettably, despite the recommendation that such criteria be routinely applied (4-6), high-profile journals continue to publish studies that do not meet the necessary controls (7), and many new researchers fail to utilize them. To publicize these standards, we summarize the key criteria below.

Physically isolated work area. To avoid contamination, it is essential that, prior to the amplification stage, all ancient DNA research is carried out in a dedicated, isolated environment. A building in which large amounts of the target DNA are routinely amplified is obviously undesirable (8).

Control amplifications. Multiple extraction and PCR controls must be performed to detect sporadic or low-copy number contamination, although carrier effects do limit

their efficacy (4, 9). All contaminated results should be reported, and positive controls should generally be avoided, as they provide a contamination risk.

Appropriate molecular behavior. PCR amplification strength should be inversely related to product size (large 500- to 1000-base pair products are unusual). Reproducible mitochondrial DNA (mtDNA) results should be obtainable if single-copy nuclear or pathogen DNA is detected. Deviations from these expectations should be justified; e.g., with biochemical data. Sequences should make phylogenetic sense.



Human paleofeces, 8000 to 500 years old, from Hinds Cave, Texas, USA, is a good source of DNA for both humans and the food they ate.

Reproducibility. Results should be repeatable from the same, and different, DNA extracts of a specimen. Different, overlapping primer pairs should be used to increase the chance of detecting numts (10) or contamination by a PCR product.

Cloning. Direct PCR sequences must be verified by cloning amplified products to determine the ratio of endogenous to exogenous sequences, damage-induced errors, and to detect the presence of numts. Overlapping fragments are desirable to confirm that sequence variation is authentic and not the product of errors introduced when PCR amplification starts from a small number of damaged templates (11).

Independent replication. Intra-laboratory contamination can only be discounted when separate samples of a specimen are extracted and sequenced in independent laboratories. This is particularly important with human remains or novel, unexpected results.

Biochemical preservation. Indirect evidence for DNA survival in a specimen can be provided by assessing the total amount, composition, and relative extent of diagenetic change in amino acids and other residues (12, 13).

Quantitation.* The copy number of the DNA target should be assessed using competitive PCR (4, 11). When the number of starting templates is low (<1,000), it may be impossible to exclude the possibility of sporadic contamination, especially for human DNA studies.

Associated remains.* In studies of human remains where contamination is especially problematic, evidence that similar DNA targets survive in associated faunal material is critical supporting evidence. Faunal remains also make good negative controls for human PCR amplifications.

We recognize that adherence to these criteria as part of routine good practice is both expensive and time-consuming. However, failure to do so can only lead to an increasing number of dubious claims, which will bring the entire field into further disrepute. If ancient DNA research is to progress and fulfill its potential as a fully-fledged area of evolutionary research, then it is essential that journal editors, reviewers, granting agencies, and researchers alike subscribe to criteria such as these for all ancient DNA research.

Alan Cooper

Departments of Zoology and Biological Anthropology, University of Oxford, Oxford OX2 6UE, UK. E-mail: alan.cooper@zoo.ox.ac.uk

Hendrik N. Poinar

Max Planck Institute for Evolutionary Anthropology, Inselstrasse 22, D-04103 Leipzig, Germany. E-mail: poinar@eva.mpg.de

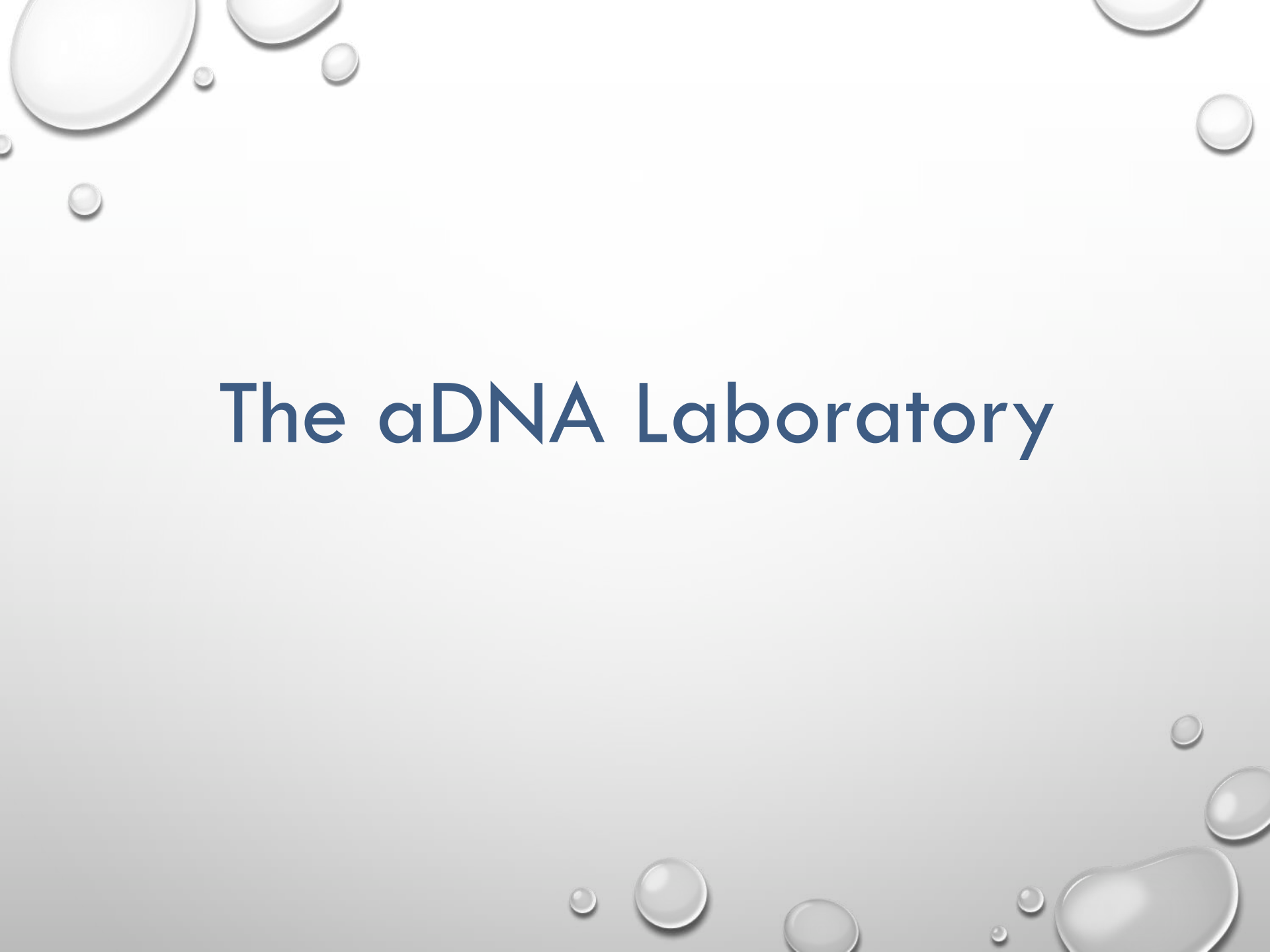
*For important discoveries, additional criteria are also essential.

References

1. J. J. Austin, A. J. Ross, A. B. Smith, R. A. Fortey, R. H. Thomas, *Proc. R. Soc. London B* 264, 467 (1997).
2. S. R. Woodward, N. J. Weyand, M. Bunnell, *Science* 266, 1229 (1994).
3. H. Zischler et al., *Science* 268, 1192 (1995).
4. O. Handt, M. Krings, R. H. Ward, S. Pääbo, *Am. J. Hum. Genet.* 59, 368 (1996).
5. A. Cooper, *Am. J. Hum. Genet.* 60, 1001 (1997).
6. R. Ward and C. Stringer, *Nature* 388, 225 (1997).
7. M. Scholz et al., *Am. J. Hum. Genet.* 66, 1927 (2000).
8. T. Lindahl, *Nature* 365, 700 (1993).
9. A. Cooper, in *Ancient DNA*, B. Herrmann and S. Hummel, Eds. (Springer-Verlag, New York, 1993), pp. 149-165.
10. A. D. Greenwood, C. Capelli, G. Possnert, S. Pääbo, *Mol. Biol. Evol.* 16, 1466 (1999).
11. M. Krings et al., *Cell* 90, 19 (1997).
12. H. N. Poinar, M. Höss, J. L. Bada, S. Pääbo, *Science* 272, 864 (1996).
13. H. N. Poinar and B. A. Stankiewicz, *Proc. Natl. Acad. Sci. U.S.A.* 96, 8426 (1999).

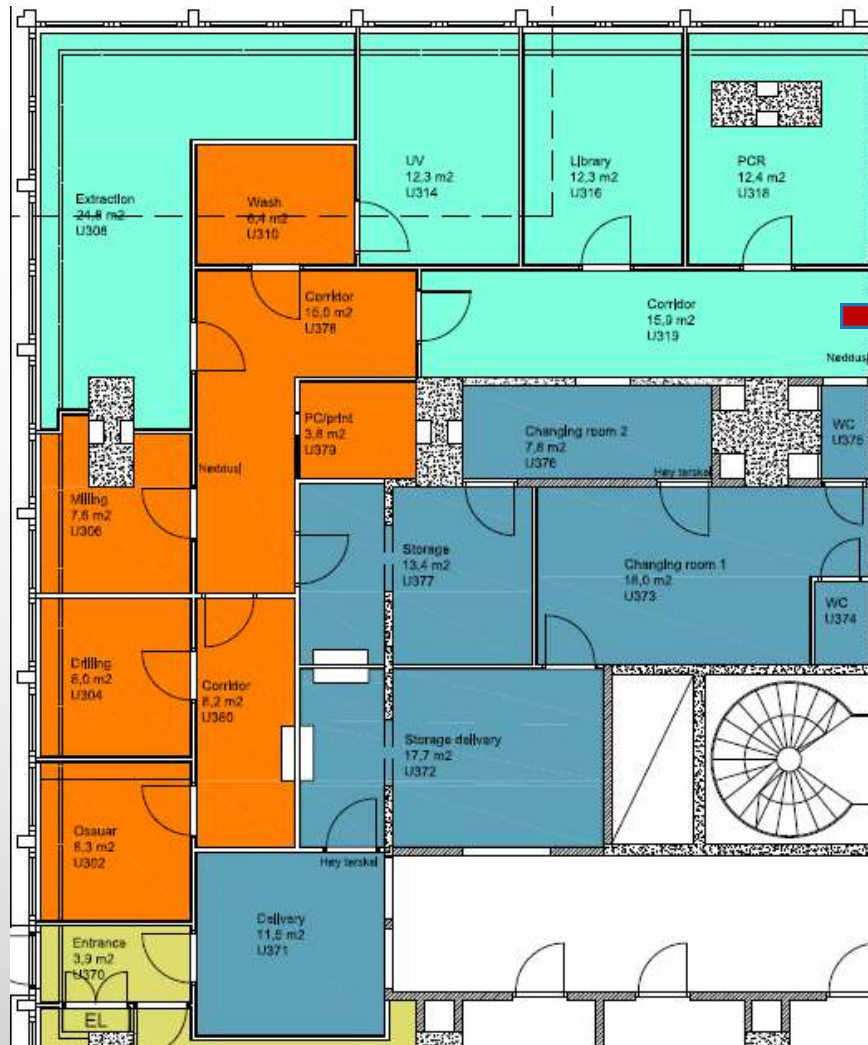
5 years later...

- Physically isolated work area
- Multiple analyses (Reproducibility)
- [Independent replication]
- Criteria for authenticity (signals of decay, phylogeny, ...)

The background of the slide is a light gray gradient. It is decorated with several realistic water droplets of various sizes, scattered in the corners. The droplets have highlights and shadows, giving them a three-dimensional appearance. The text is centered in the middle of the slide.

The aDNA Laboratory

The aDNA lab at CEES in Oslo



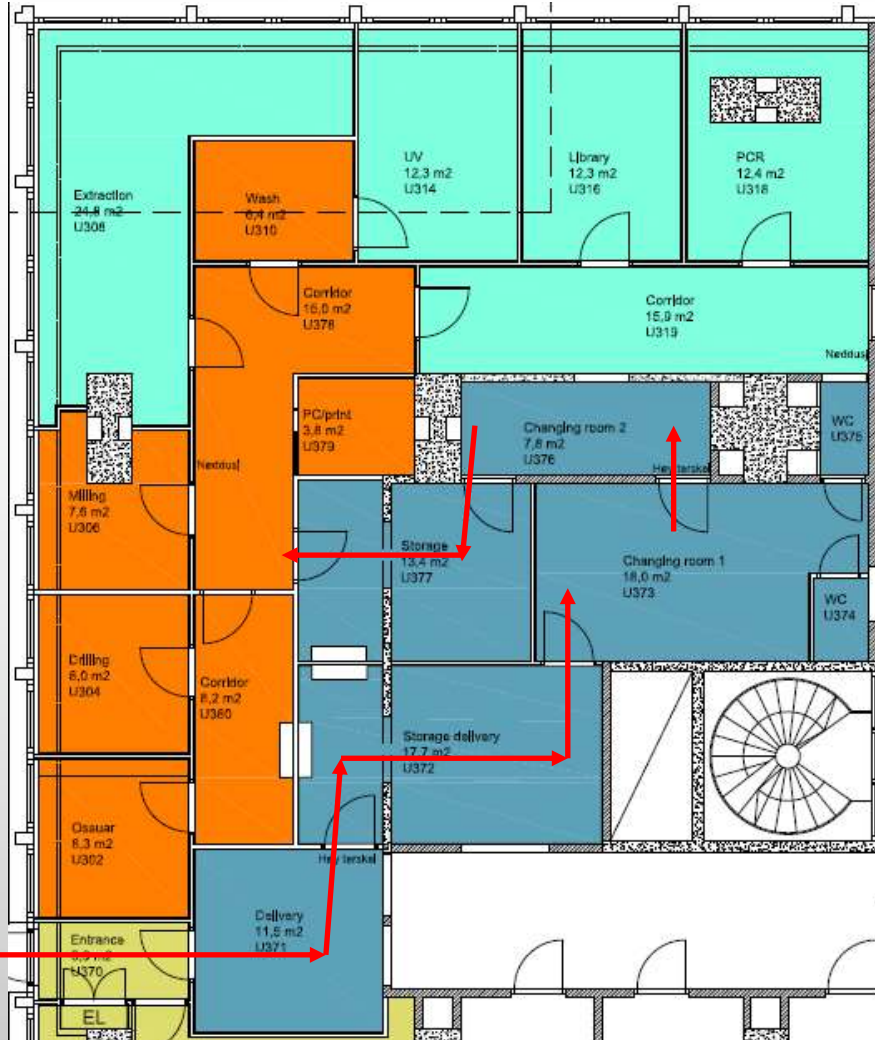
Entrance with
Special Key



Emergency exit

- ❖ Only authorised workers are allowed to enter the lab after a special training.
- ❖ Independent entrance
- ❖ Separate ventilation system with positive pressure.

The aDNA lab at CEES in Oslo



Shower and fresh washed clothes.



Wear protective clothes.



Leave your clothes in the lockers.



Leave your pieces of external clothes in the lockers.

Inside the lab

aDNA worker's outfit and behaviour:

1. one-way rule, freshly showered and freshly washed clothes, direct way, never entering building with offices and other labs prior to aDNA lab

2. cover skin, prevent loss of eyelashes and hair in the lab to protect aDNA-lab environment from worker's DNA:

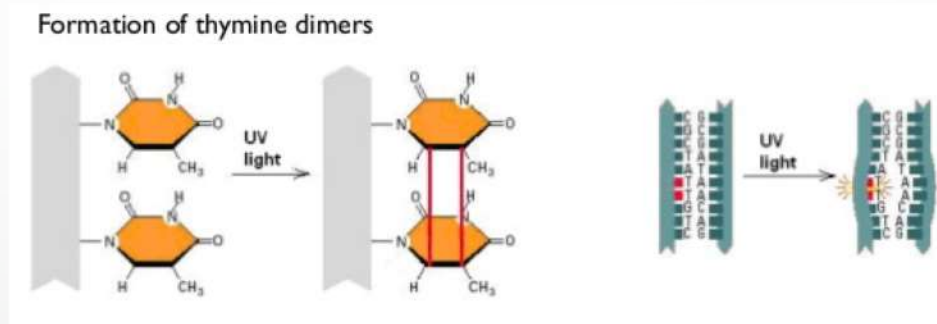
- Caps/medical head wear
- Surgical facemask
- Helmet and visor
- Overall
- 2-3 pairs of gloves
- Overshoes

3. Keep Clean!



UV-irradiation

- Produce dimers between two consecutive pyrimidines (especially between two thymines)
- Results in **inhibition of the PCR-reaction**



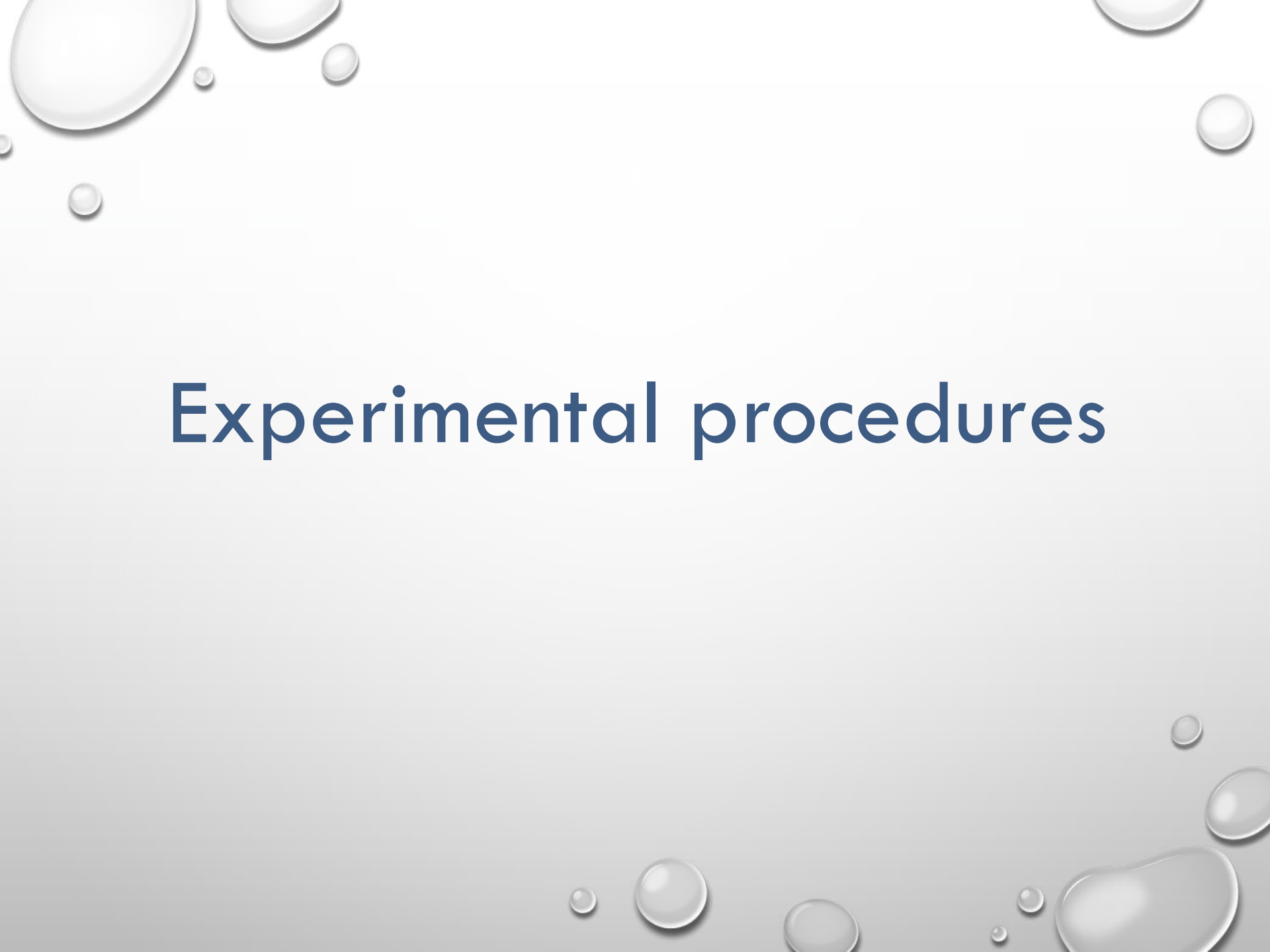
UV-irradiation of all disposables and working area



UV-irradiation of samples



Even water for cleaning is UV-irradiated!

The background of the slide is a light gray gradient. It is decorated with several realistic water droplets of various sizes, scattered in the corners. The droplets have highlights and shadows, giving them a three-dimensional appearance. The largest droplets are in the top-left and bottom-right corners, while smaller ones are scattered throughout.

Experimental procedures

Advices for Sampling

- ❖ Wear protective clothes by handling even in the repository (at least gloves and face mask)
- ❖ Don't wash the samples for aDNA analyses!!!
- ❖ Don't use glue or other chemicals!!!
- ❖ Don't write on the specimens!!! Use bags.
- ❖ **If possible, isolate two samples of each individual for aDNA analyses during the excavation**
- ❖ **Take contact with an accredited aDNA expert for advices asap**



Work-flow



Introduction
in the
aDNA-Lab



Cataloging & UV



Sandblasting



Milling



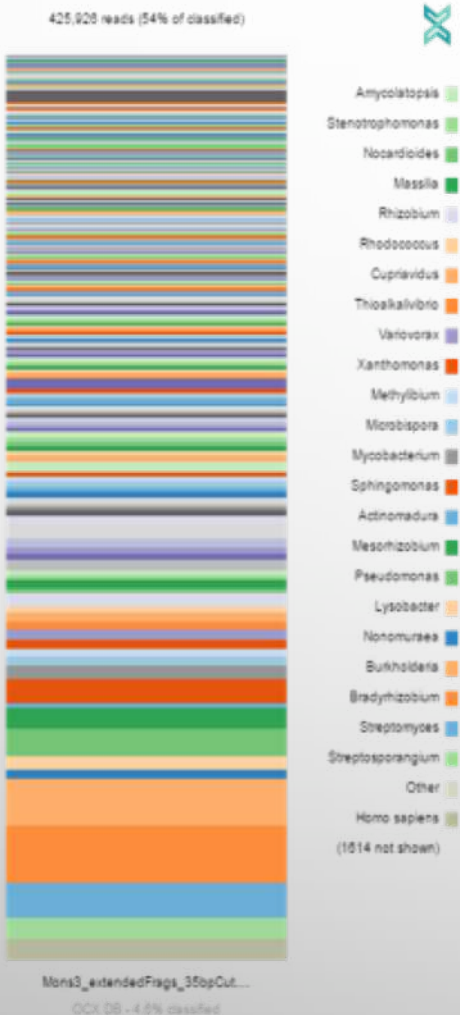
Preparation of
PCRs and
libraries for
sequencing



Extraction

Shotgun Sequencing (Metagenomic analysis)

(outside the aDNA)

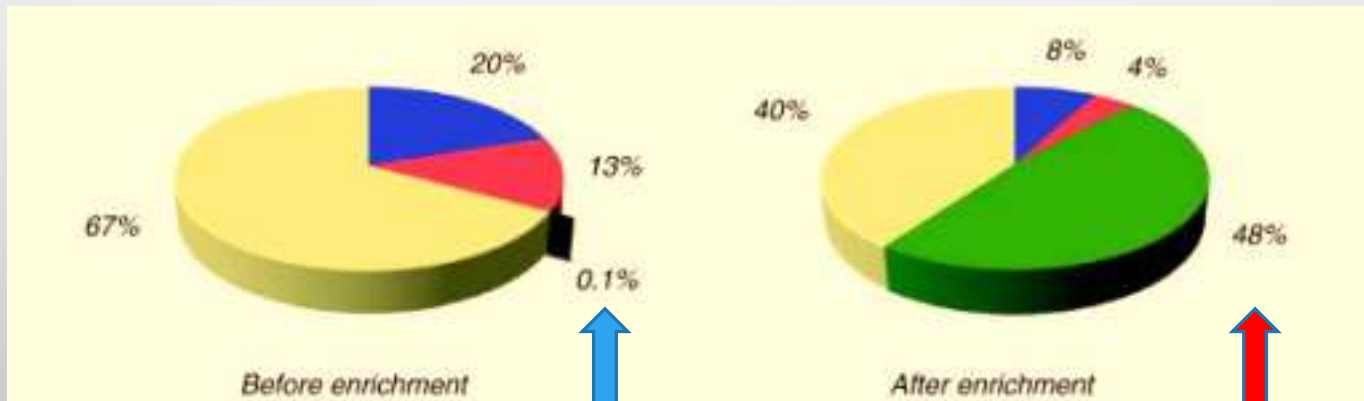


Whole collection
of genomes
isolated from a
sample.

Endogen DNA 1% !!

Target enrichment (Capture) & Sequencing

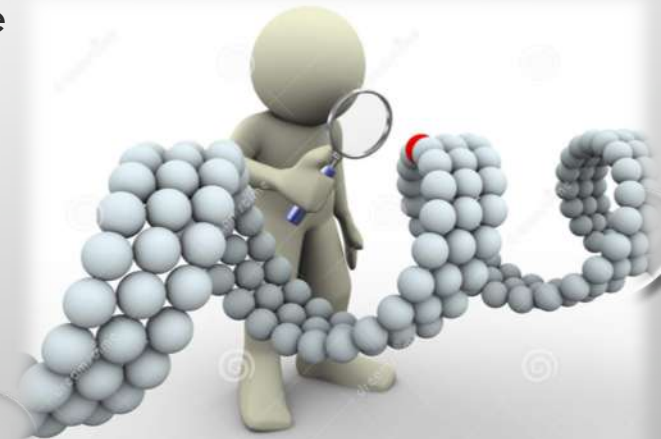
(outside the aDNA)



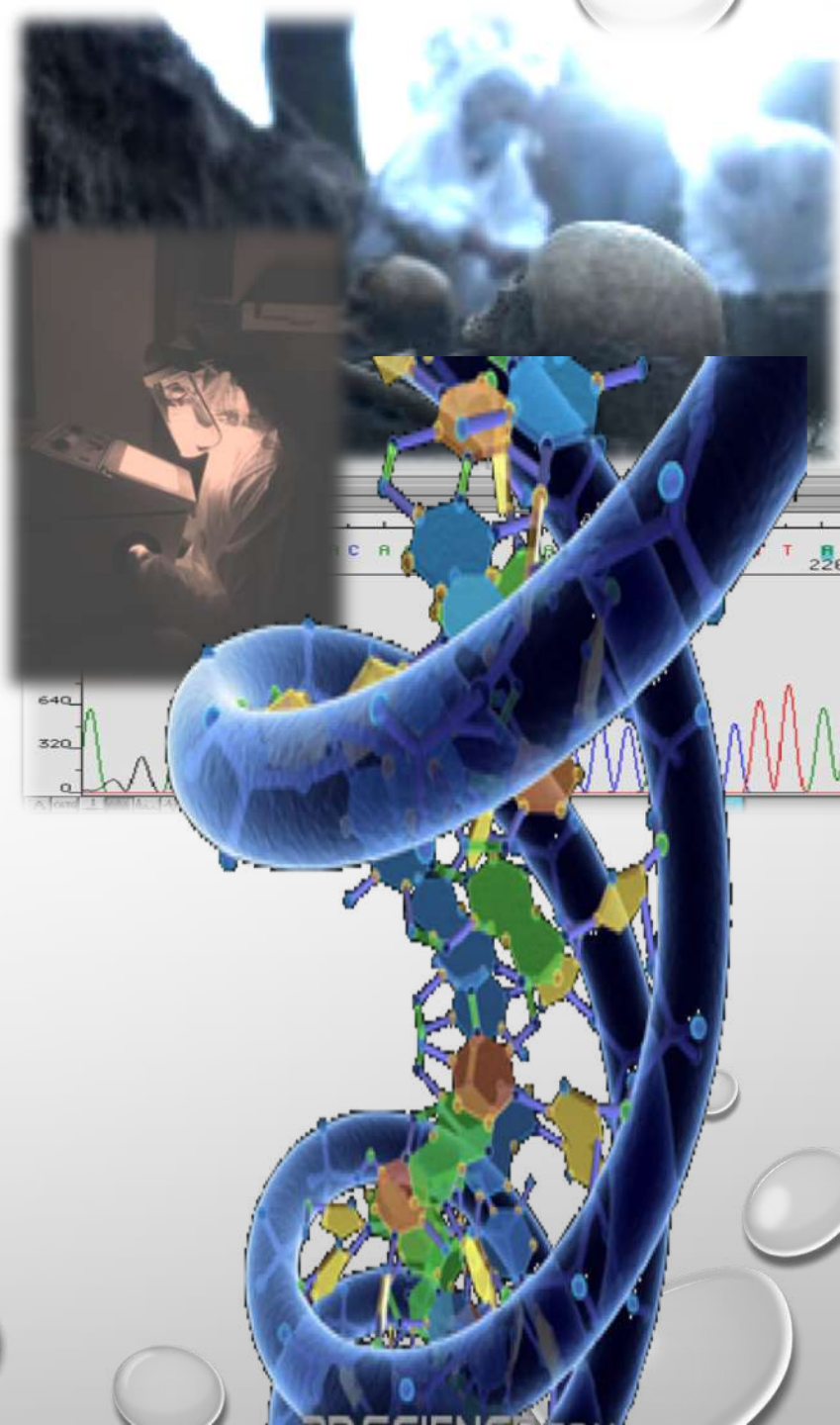
(Bioinformatic work

- Loading reads (+ quality info).
- Loading reference sequence(s).
- Demultiplexing (sorting the reads into different files according to their indexes).
- Paired end splitting (sorting for reads sequenced in two directions).
- Trimming (adapters) and filtering of reads according to various quality criteria (for instance length).
- Calculating global statistics on the project.
- Aligning the reads against the reference sequence(s).
- SNPs (or SNVs) calling.
- BLASTing

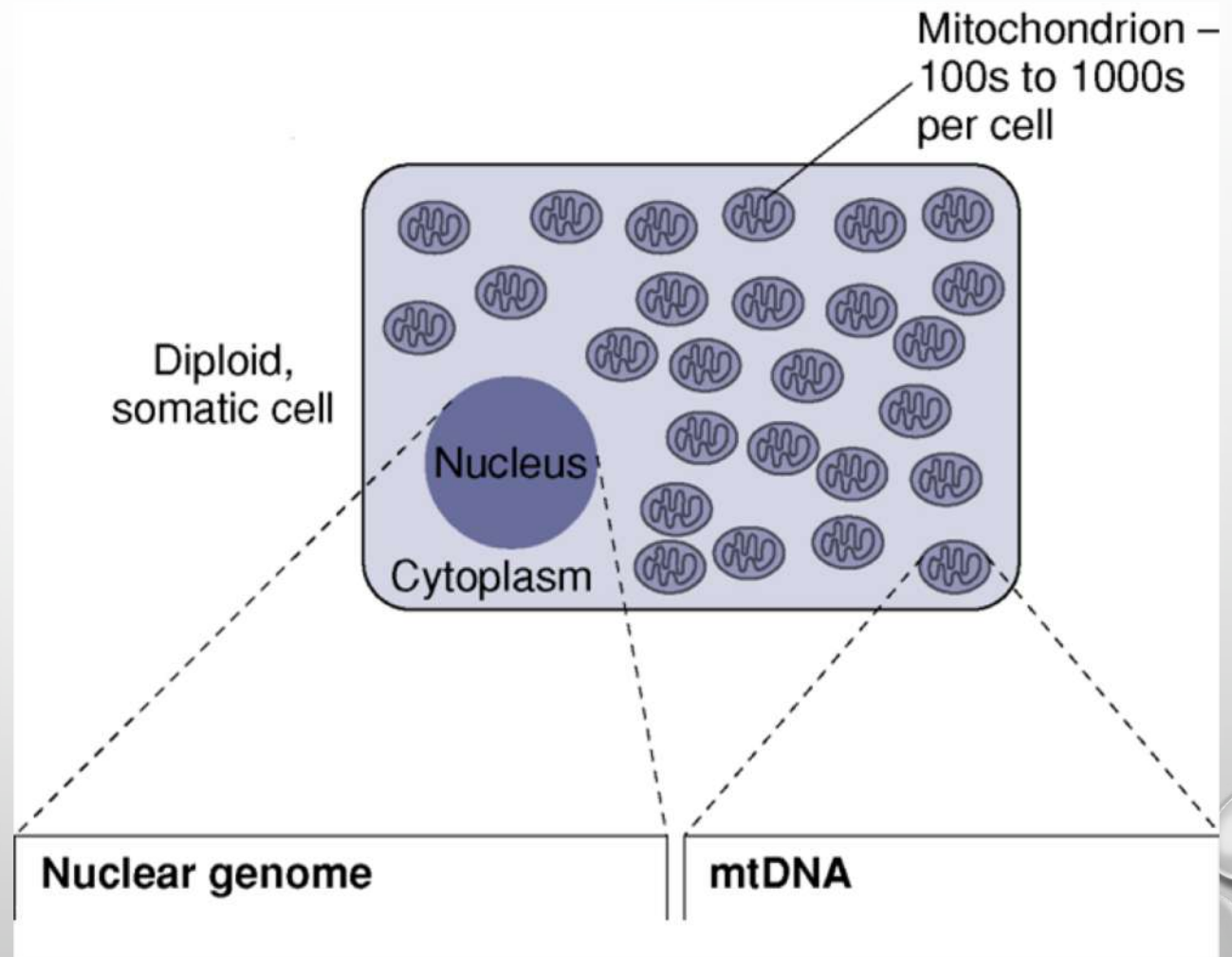
•...)



Some
examples of
aDNA
analysis from
human
remains

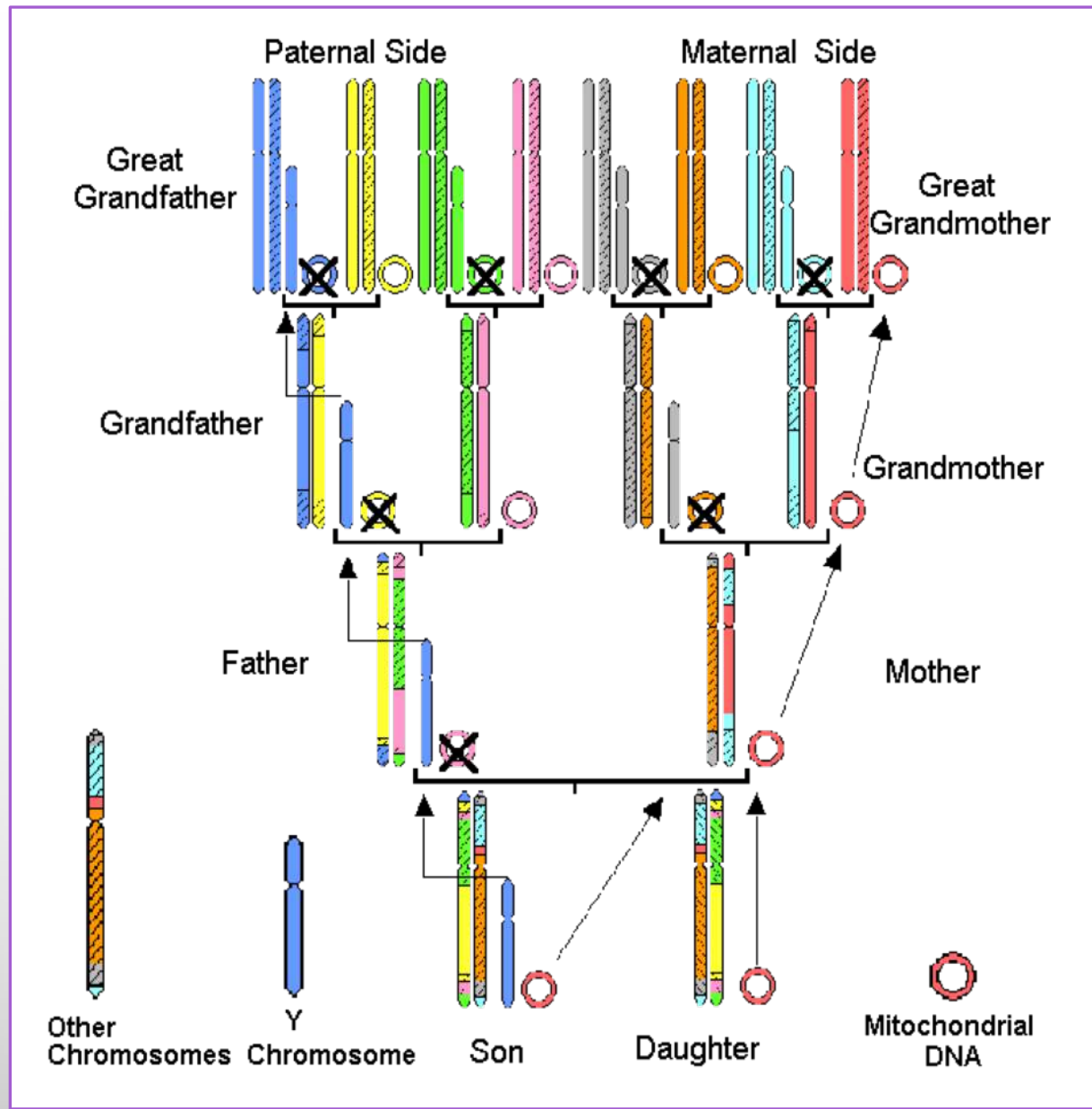


Sources of aDNA in mammalian cells



Nuclear genomic DNA vs. mtDNA

No recombination!



Attribution of skeletal elements

Westerhausen, Iron Age (ca. 270 CE).

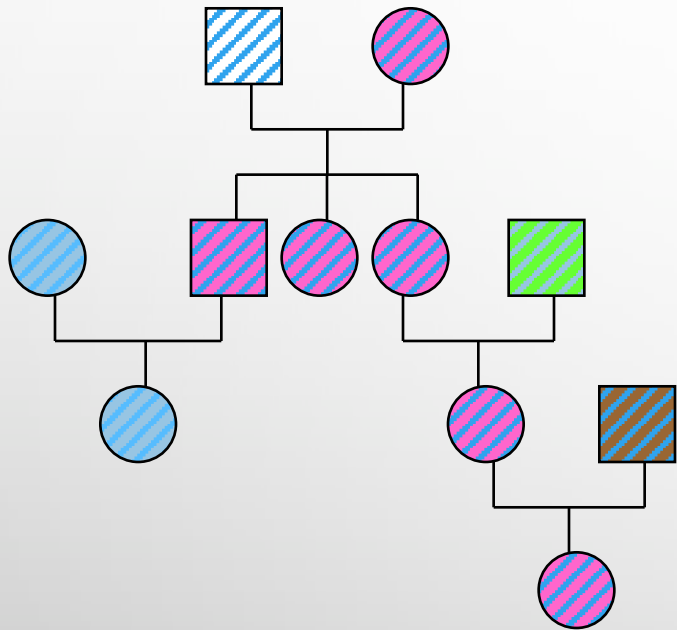


- ❖ Nine individuals, nine mtDNA haplotypes
- ❖ No maternal relationship
- ❖ Reconstruction of the individual skeletons
- ❖ nDNA confirmed the gender (8 male, 1 female ind.)

Identification and Family reconstruction

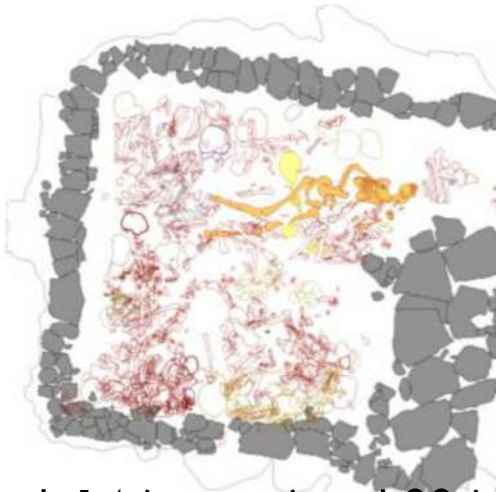
The Romanov

Maternal lineage



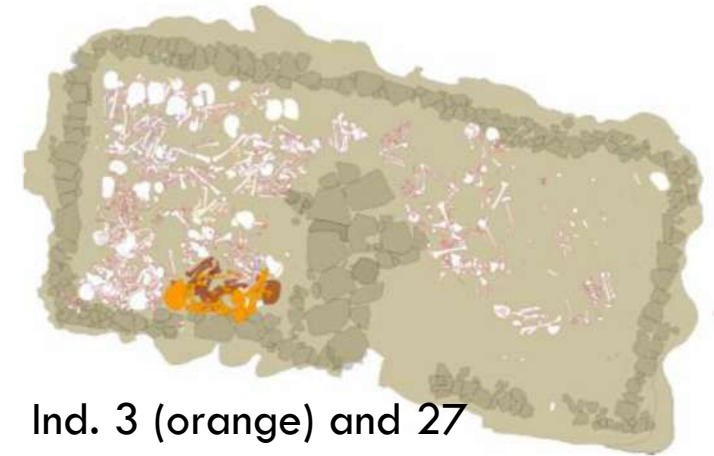
The relatives of Benzingerode

Bernburg culture (BEC), 3100 cal BC; mtDNA from 17 out of 21 individuals

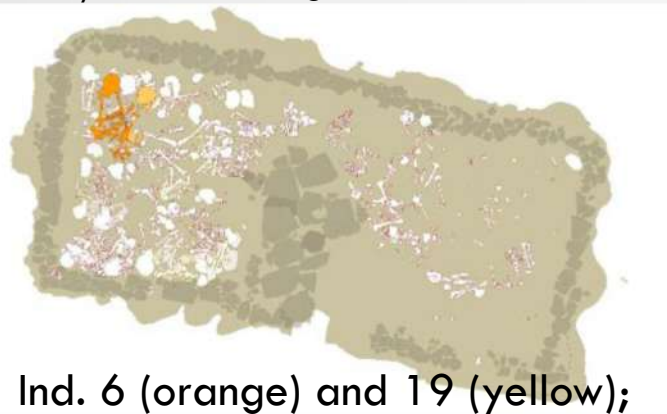


Ind. 14 (orange) and 20 (yellow);
child/mother or grandma

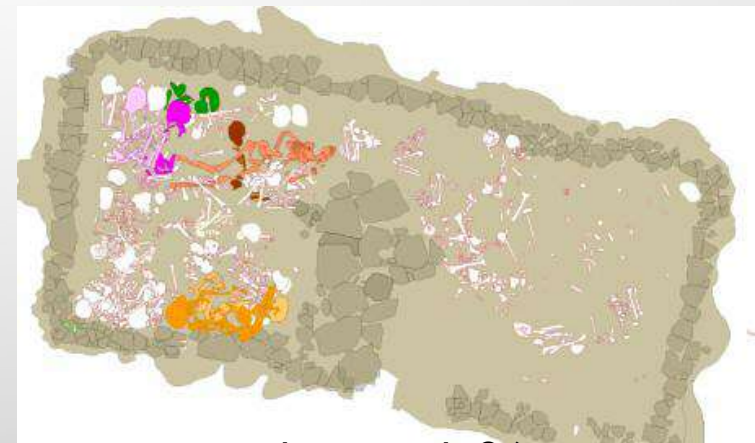
Haplotyp	Ind.	Haplogruppe
1.	1	U
2.	14, 20	
3.	35	
4.	18	
5.	3, 27	K
6.	33	T
7.	6, 19	
8.	17, 36	
9.	29	H
10.	40	
11.	39	V ?
12.	15	W
13.	37	X



Ind. 3 (orange) and 27
(brown); sibs or cousins

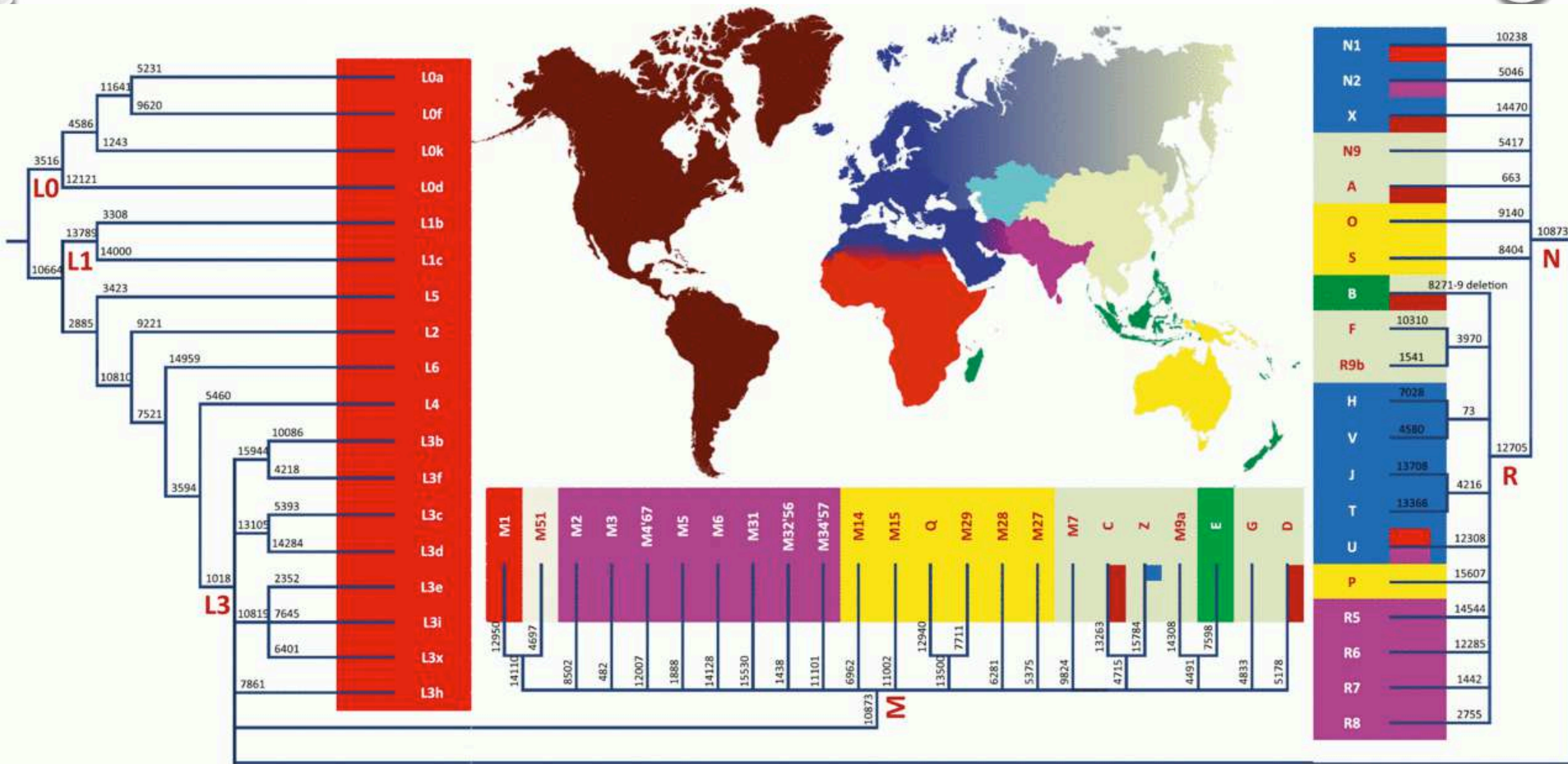


Ind. 6 (orange) and 19 (yellow);
daughter/mother or grandma;
sibs or cousins



In green ind. 17; ind. 36 was separated.

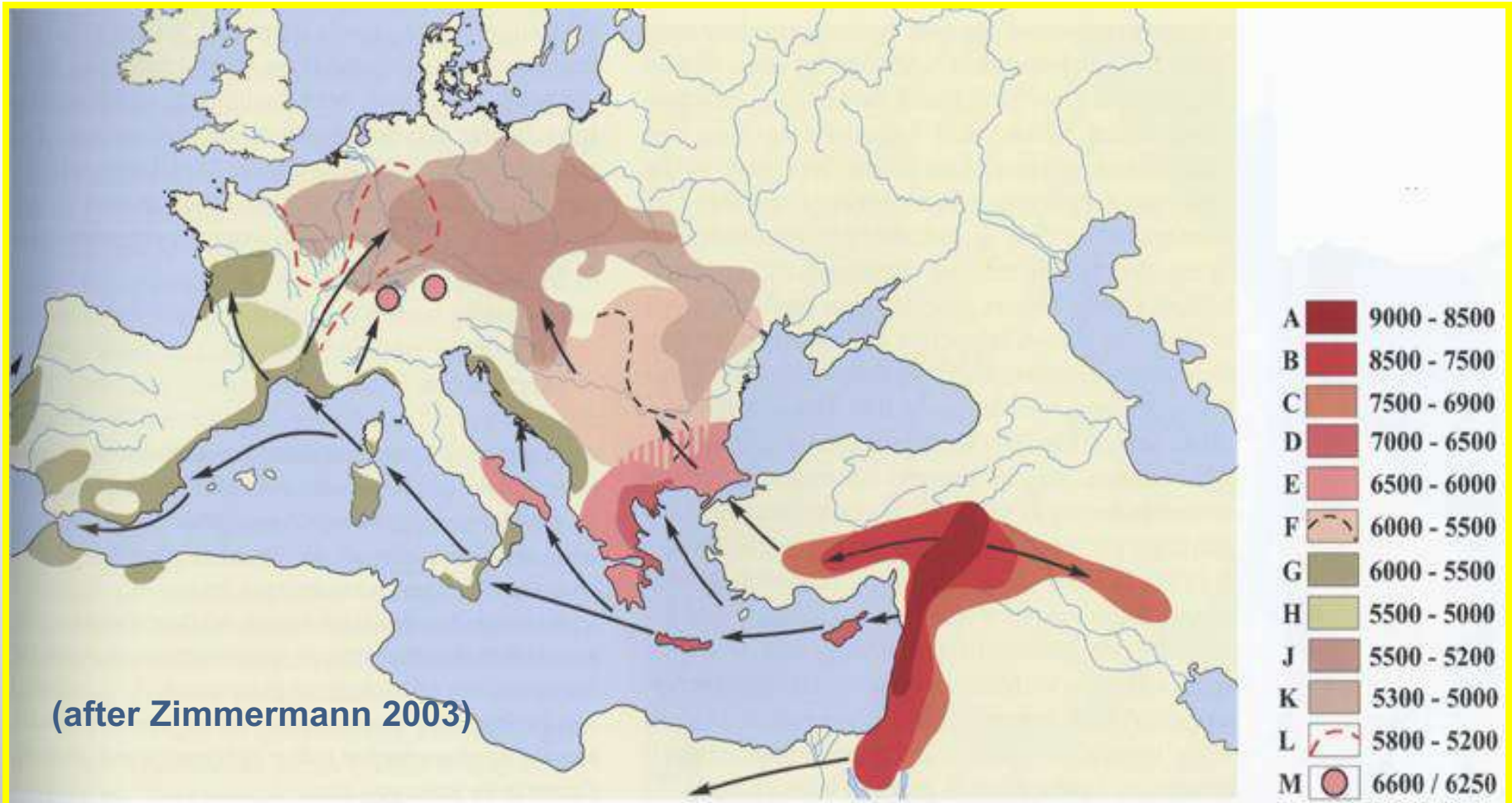
PHYLOGENETIC TREES and PEOPLING OF THE WORLD at different TIMES

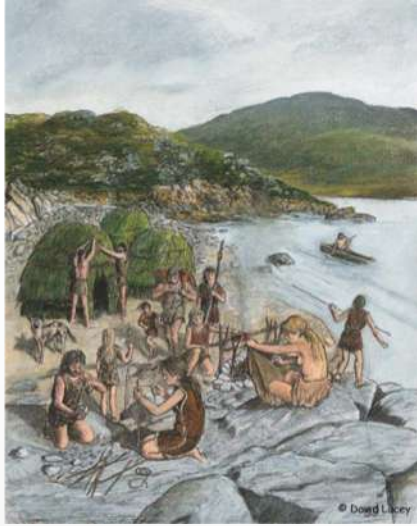


By Toomas Kivisild - Toomas Kivisild. Maternal ancestry and population history from whole mitochondrial genomes. Investigative Genetics 2015;6:3 DOI: 10.1186/s13323-015-0022-2
<http://investigativegenetics.biomedcentral.com/articles/10.1186/s13323-015-0022-2>, CC BY 2.0,
<https://commons.wikimedia.org/w/index.php?curid=50349268>

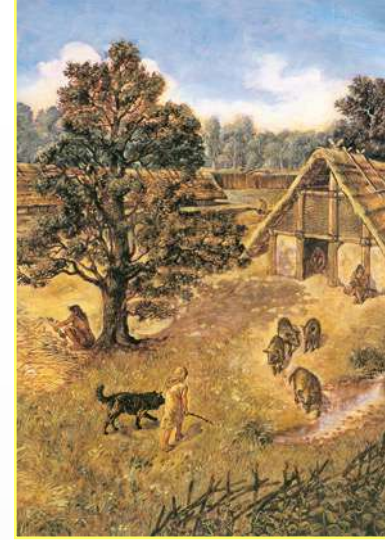
Population Genetics

The Neolithic Transition was due to migrations?





Acculturation or immigration



Hunter-gatherers (Palaeo-Mesolithic periods) 45,000-4,000 YBP

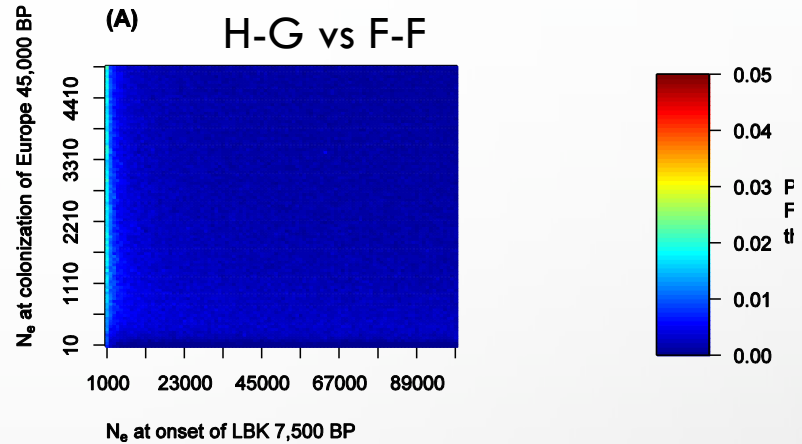
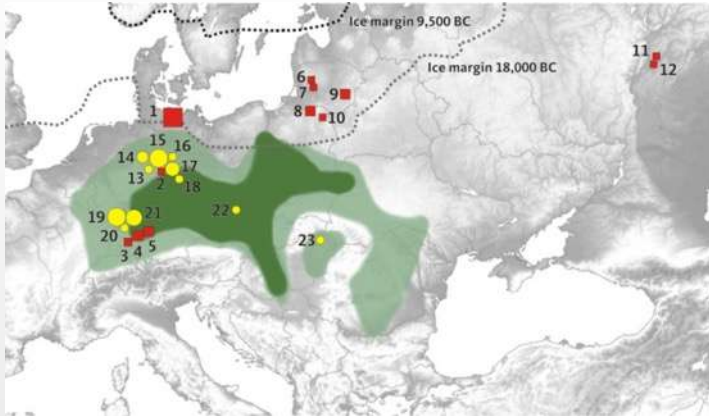
- Hunting
- Fishing
- Gathering
- Nomadism (tents or portable shelters)



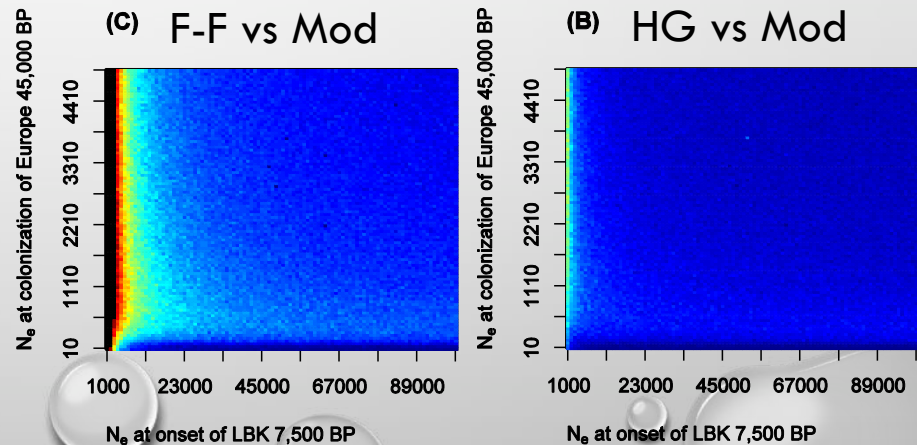
Farmers (Neolithic period) 10,000-4,000 YBP

- Use of pottery
- Agriculture
- Animal husbandry
- “Urbanisation”
- Social structures
- Technology

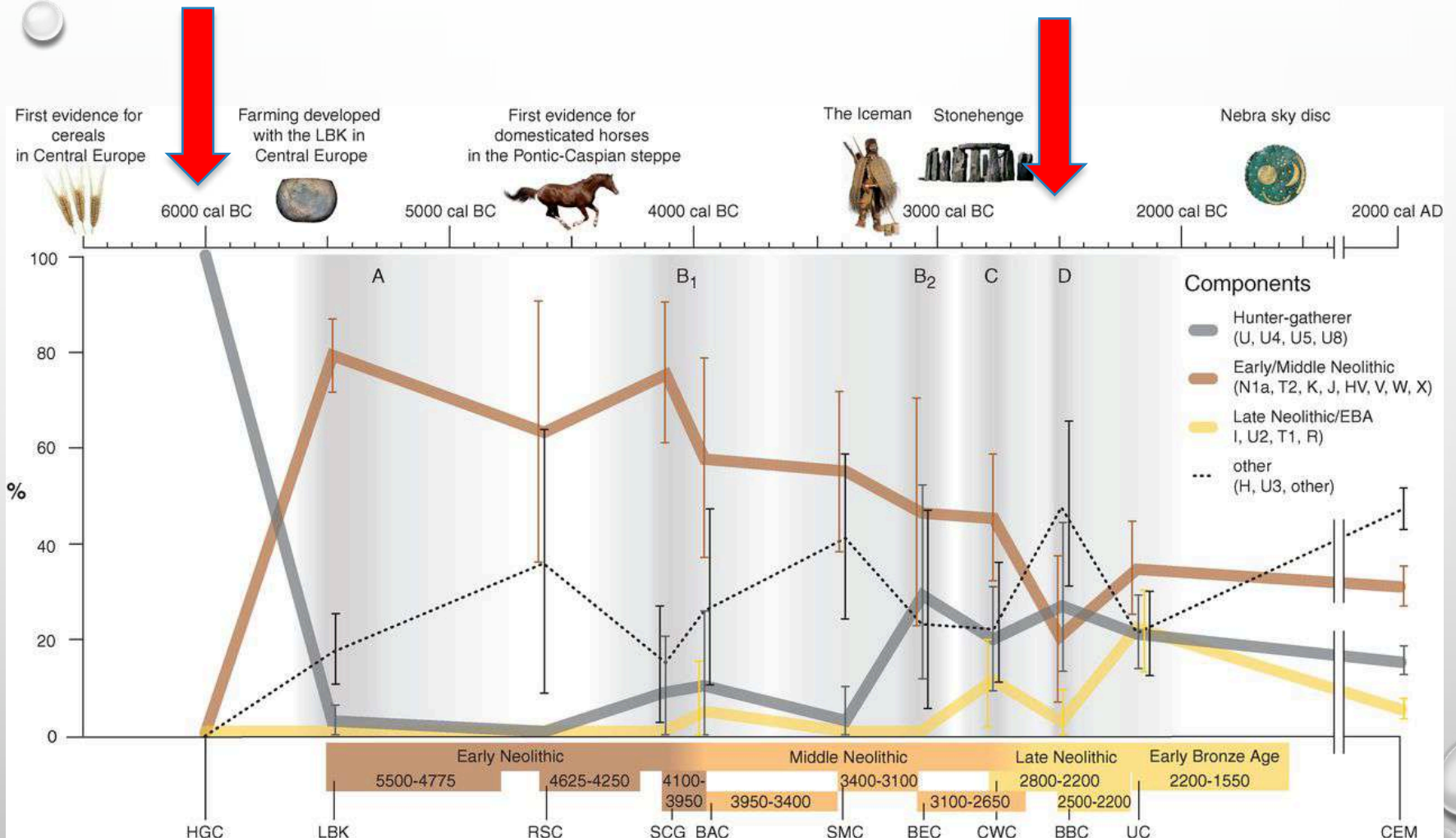
1) No genetic continuity between Hunter-Gatherers (U4 & U5) & First Farmers (other haplogroups)



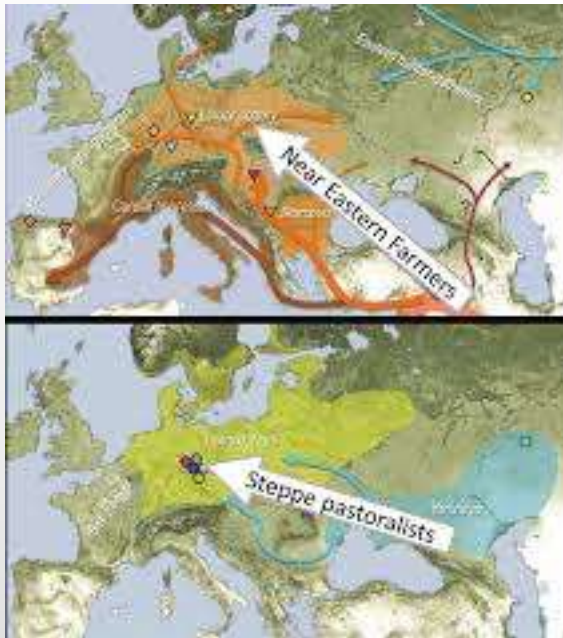
2) No direct genetic continuity between Hunter-Gatherers, First Farmers and modern Europeans



H-G and Farmers in Central Europe

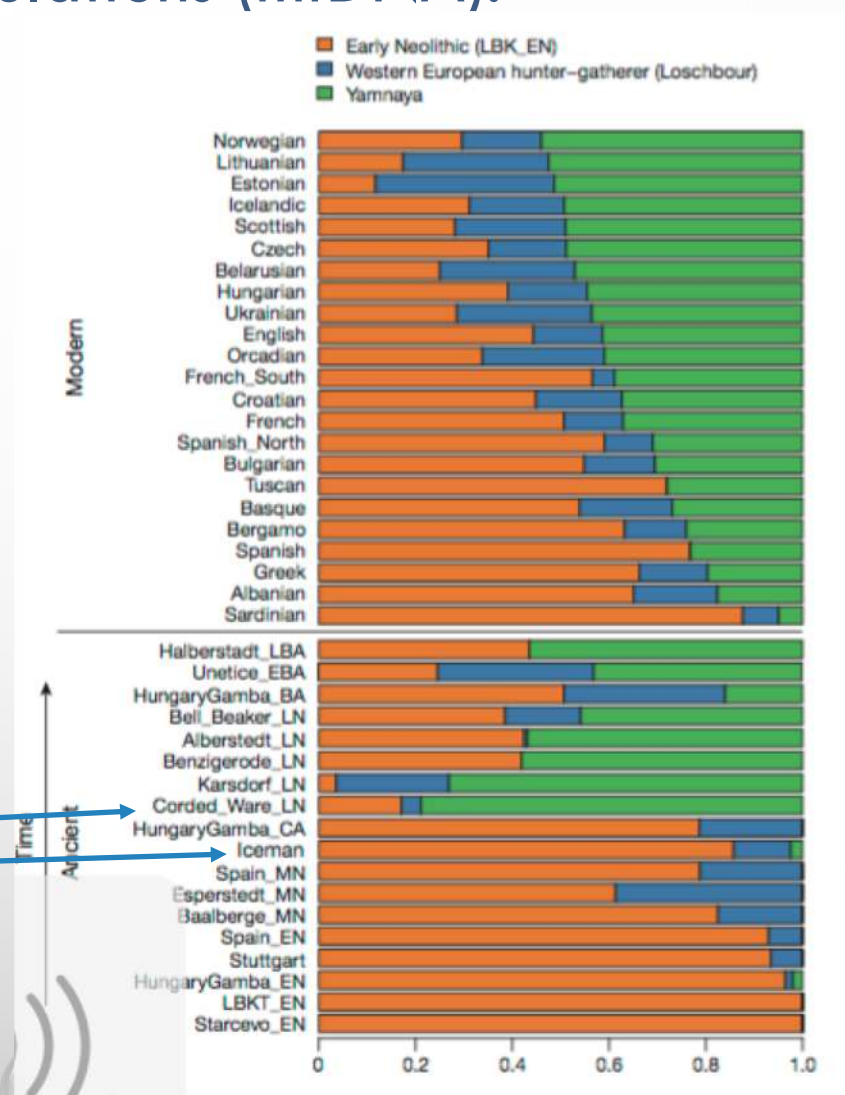


Today Europeans are a mixture of at least three different ancestral populations (mtDNA).



2400 BCE
3200 BCE

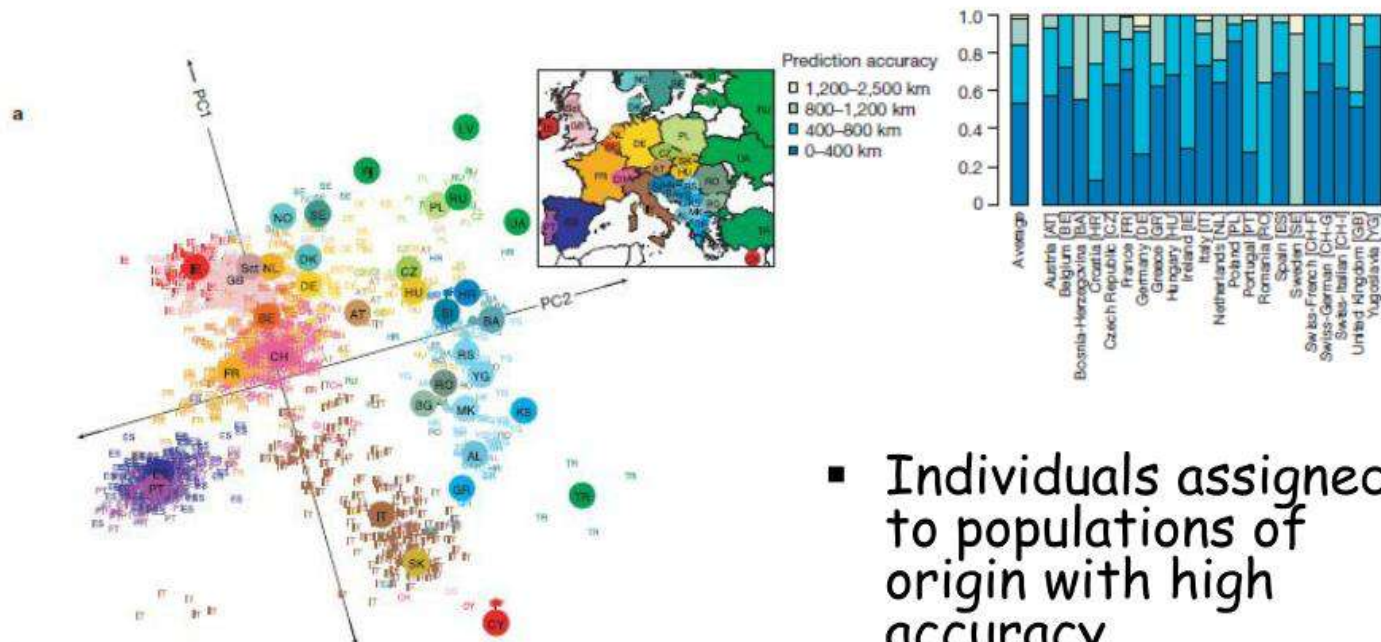
Admixture proportion inferred in ancient and modern samples (Haak et al. 2015).



Determination of individual origins (nDNA)

Human Population Assignment with SNP

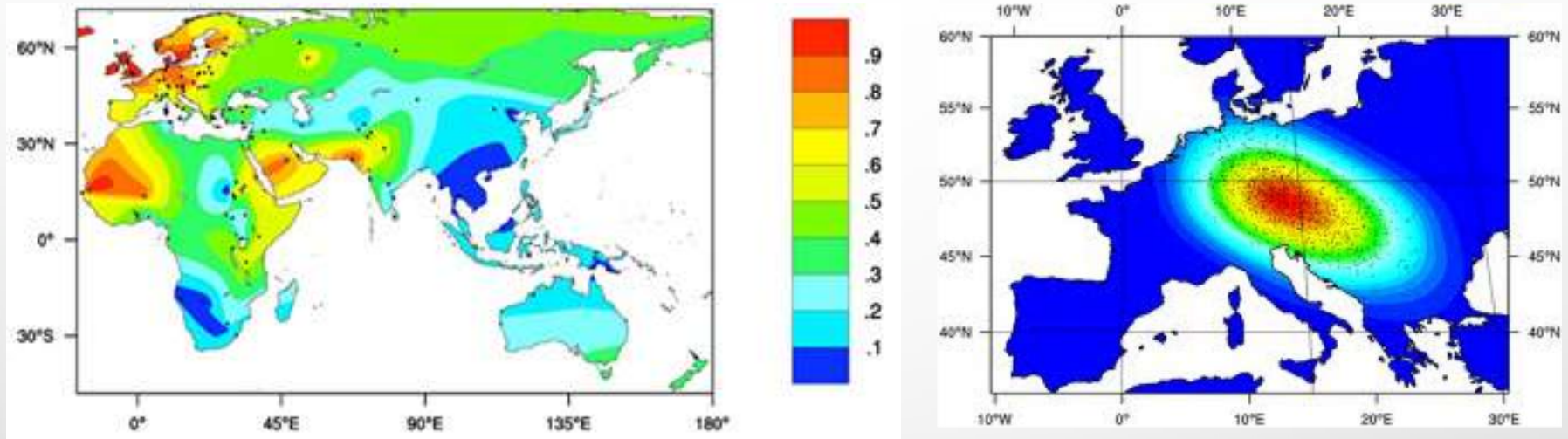
- Assayed 500,000 SNP genotypes for 3,192 Europeans
- Used Principal Components Analysis to ordinate samples in space
- High correspondence between sample ordination and geographic origin of samples



- Novembre et al. 2008 Nature 456:98

Genetic disorders & particularities (nDNA)

Lactase-persistence



Absence of the lactase-persistence-associated allele in early Neolithic Europeans

J. Burger^{1†}, M. Kirchner¹, B. Bramanti¹, W. Haak¹, and M. G. Thomas²

¹Johannes Gutenberg University, Institute of Anthropology, Saarstrasse 21, D-55099 Mainz, Germany; and ²Department of Biology, University College London, Wolfson House, 4 Stephenson Way, London NW1 2HE, United Kingdom

Edited by Walter Bodmer, Cancer Research UK, Oxford, United Kingdom, and approved December 27, 2006 (received for review September 4, 2006)

Lactase persistence (LP), the dominant Mendelian trait conferring the ability to digest the milk sugar lactose in adults, has risen to high frequency in central and northern Europeans in the last 20,000 years. This trait is likely to have conferred a selective advantage in individuals who consume appreciable amounts of unfermented

would have provided a selective advantage in the absence of a supply of fresh milk, and because of observed correlations between the frequency of LP and the extent of traditional reliance on animal milk, the culture-historical hypothesis has been proposed (8–12). Under this model, LP was driven from

Itan et al. 2009
(Burger et al. 2007,
Malmström et al. 2010
Sverrisdottir et al. 2014)

...

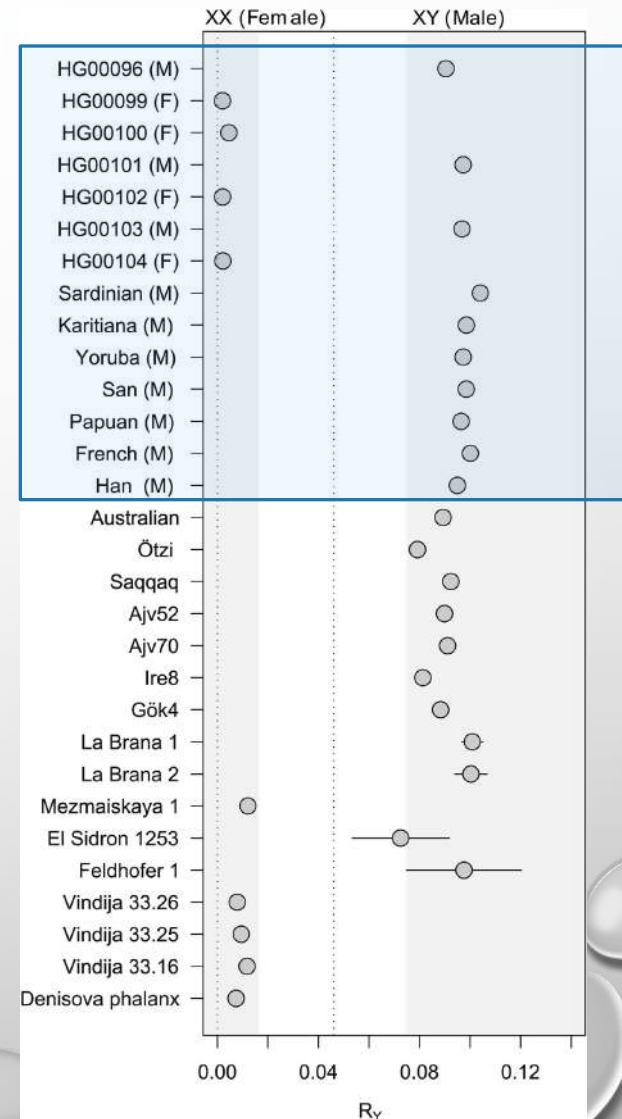
Determination of sex (nDNA)

Metodo di Skoglund

(et al. 2013):

„even relatively **sparse shotgun sequencing (about 100,000 human sequences)** can be used to reliably identify chromosomal sex simply by considering the **ratio of sequences aligning to the X and Y chromosomes**“.

- Also in subadults
- Also on fragmented bones (no skull, no pelvis)
- Most accurate

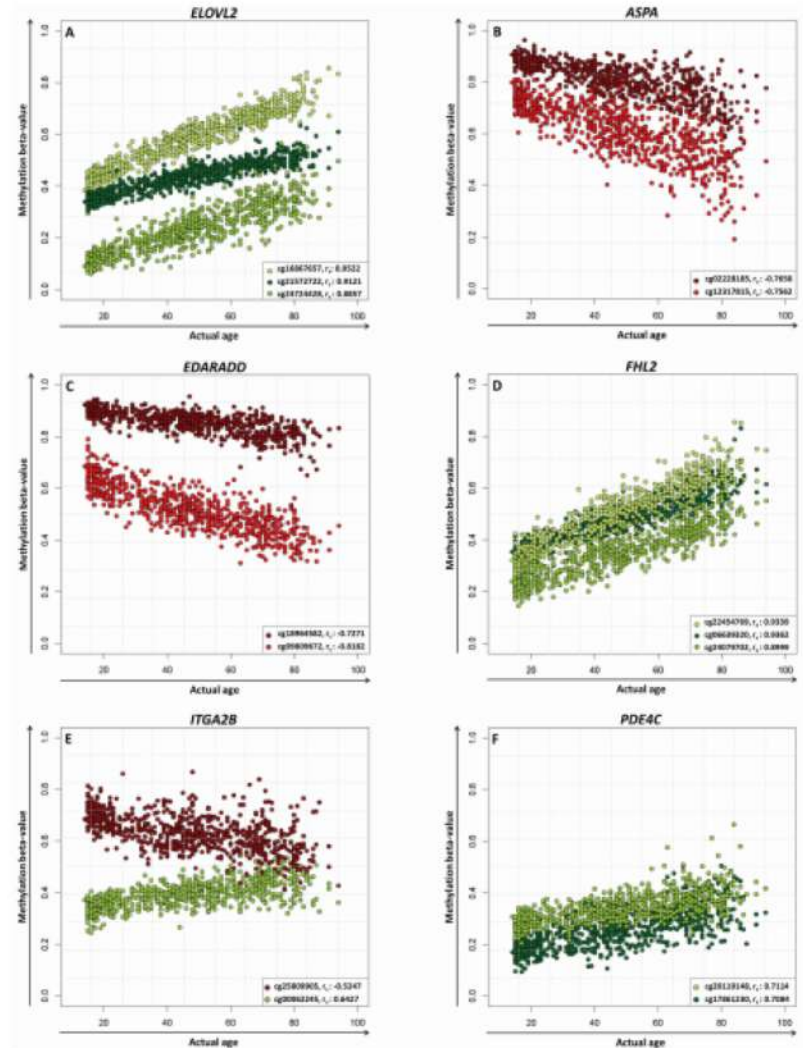
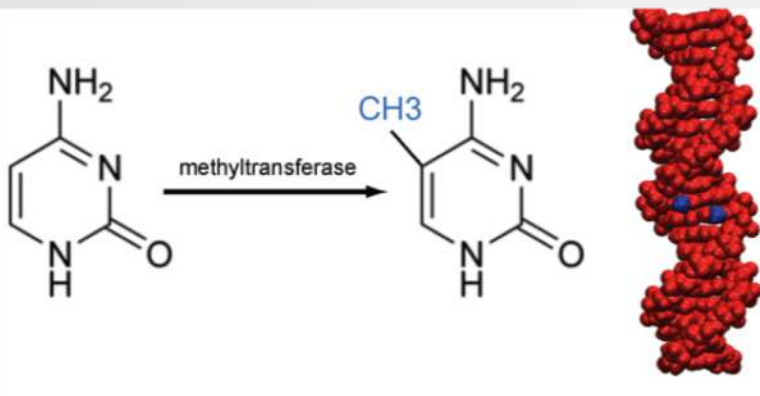
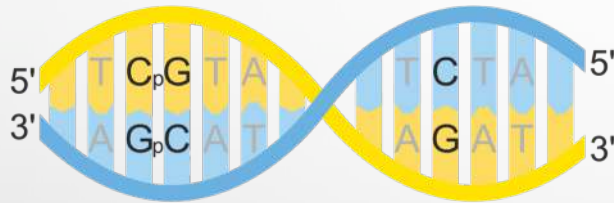


Individual Age Estimation (Forensic Anthr.)

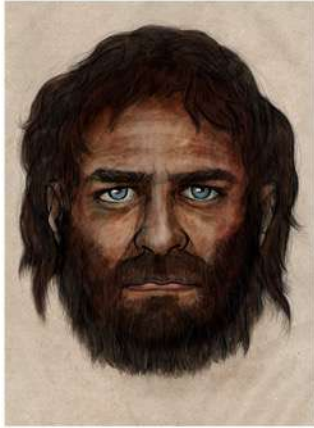
„CpG sites hypermethylated with age are plotted in green shades, whereas red tones correspond to hypomethylated positions.“

EPIGENETICS

studies gene-regulation (often silencing) due to Methylation of the CpGs
In mammals, 70% - 80% of all CpGs are methylated.



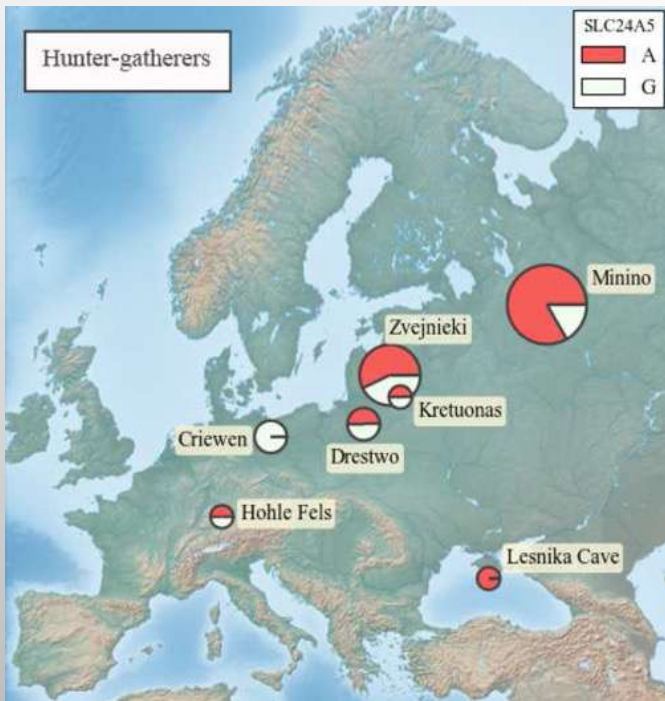
Somatic traits (nDNA)



La Braña 1, a 7,000-year-old individual from the Mesolithic Period, had blue eyes and dark skin. Credit: Spanish National Research Council

La Braña 1 has a common ancestor with the settlers of the Upper Paleolithic site of Mal'ta, located in Lake Baikal (Siberia)

Olalde et al. 2014
(Wilde et al. 2014)



Kirsanow et al. unpublished
(85 prehistoric and 138
historic individuals analysed)

Contents lists available at ScienceDirect

Forensic Science International: Genetics

journal homepage: www.elsevier.com/locate/fsigen

Research paper

The HirisPlex-S system for eye, hair and skin colour prediction from DNA: Introduction and forensic developmental validation

Lakshmi Chaitanya^a, Krystal Breslin^b, Sofia Zuñiga^c, Laura Wirken^d, Ewelina Pośpiech^e, Magdalena Kukla-Bartoszek^f, Titia Sijen^g, Peter de Knijff^h, Fan Liu^{a,g,h,i}, Wojciech Branicki^{e,i}, Manfred Kayser^{a,b,i}, Susan Walsh^{b,i}

^a Department of Genetic Identification, Erasmus MC University Medical Centre Rotterdam, Rotterdam, The Netherlands
^b Department of Biology, Indiana University Purdue University Indianapolis (IUPUI), IN, USA
^c Division Biological Traces, Netherlands Forensic Institute, The Hague, The Netherlands
^d Forensic Laboratory for DNA Research, Department of Human Genetics, Leiden University Medical Center, Leiden, The Netherlands
^e Malopolska Centre of Biotechnology, Jagiellonian University, Kraków, Poland
^f Faculty of Biochemistry, Biophysics and Biotechnology of the Jagiellonian University, Kraków, Poland
^g Key Laboratory of Genomic and Precision Medicine, Beijing Institute of Genomics, Chinese Academy of Sciences, Beijing, China
^h University of Chinese Academy of Sciences, Beijing, China
ⁱ Central Forensic Laboratory of the Police, Warsaw, Poland

Check for updates

Microbioma and diet



Jensen et al. 2019

Lola's portrait, “reconstructed” by a 5,700 years old chewing-gum (chewed birch pitch) – no human bones!

- Entire genome
- Oral microbiome
- Meal (hazelnuts and mallard duck but no milk)



(Illustration by Tom Björklund)

Distinct Clones of *Yersinia pestis* Caused the Black Death

Stephanie Haensch¹, Raffaella Bianucci^{2,3}, Michel Signoli^{3,4}, Minoarisoa Rajerison⁵, Michael Schultz⁶, Sacha Kacki^{7,8}, Marco Vermunt⁹, Darlene A. Weston^{10,11,12}, Derek Hurst¹³, Mark Achtman¹⁴, Elisabeth Carniel¹⁵, Barbara Bramanti^{1*}

1 Institute for Anthropology, Johannes Gutenberg University, Mainz, Germany, **2** Laboratory of Criminalistics Sciences Department of Anatomy, Pharmacology and Legal Medicine, University of Turin, Turin, Italy, **3** Unité d'Anthropologie Bioculturelle, Faculté de Médecine, Université de Montpellier-CHU-FES, Montpellier, France, **4** Centre d'Études Préhistoriques, Antiquités, Moyen-Âge, UMR 6133 CNRS-286 University of Nice, Valbonne, France, **5** Center for Plague, Institute Pasteur de Madagascar, World Health Organization Collaborating, Antananarivo, Madagascar, **6** Department of Anatomy and Embryology, Medical Faculty, Georg-August University, Göttingen, Germany, **7** UMR, Villeveuve d'Asco, Archeological Center, Villeveuve d'Asco, France, **8** Laboratoire d'Anthropologie des Populations du Pasé, Université Bordeaux 1, Talence, France, **9** Department of Manuscripts and Archaeology, Municipality of Bergen op Zoom, Bergen op Zoom, The Netherlands, **10** Biogen Anthropology, Department of Anatomy and Embryology, Leiden University Medical Center, Leiden, The Netherlands, **11** Division of Archaeological Sciences, University of Bradford, Bradford, West Yorkshire, United Kingdom, **12** Department of Human Evolution, Max Planck Institute for Evolutionary Anthropology, Leipzig, Germany, **13** Worcestershire Historic Environment and Archaeology Service, Worcestershire County Council, Worcester, United Kingdom, **14** Environmental Research Institute, University College Cork, Cork, Ireland, **15** Viriditas Research Unit, Institut Pasteur, Paris, France

Abstract

From AD 1347 to AD 1353, the Black Death killed tens of millions of people in Europe, leaving misery and devastation in its wake, with successive epidemics ravaging the continent until the 18th century. The etiology of this disease has remained highly controversial, ranging from claims based on genetics and the historical descriptions of symptoms that it was caused by *Yersinia pestis* to conclusions that it must have been caused by other pathogens. It has also been disputed whether plague had the same etiology in northern and southern Europe. Here we identified DNA and protein signatures specific for *Y. pestis* in human skeletons from mass graves in northern, central and southern Europe that were associated archaeologically with the Black Death and subsequent resurgences. We confirm that *Y. pestis* caused the Black Death and later epidemics on the entire European continent over the course of four centuries. Furthermore, on the basis of 17 single nucleotide polymorphisms plus the absence of a deletion in *gloD* gene, our aDNA results identified two previously unknown but related clades of *Y. pestis* associated with distinct medieval mass graves. These findings suggest that plague was imported to Europe on two or more occasions, each following a distinct route. These two clades are ancestral to modern isolates of *Y. pestis* biovars Orientalis and Medievalis. Our results clarify the etiology of the Black Death and provide a paradigm for a detailed historical reconstruction of the infection routes followed by this disease.

Citation: Haensch S, Bianucci R, Signoli M, Rajerison M, Schultz M, et al. (2010) Distinct Clones of *Yersinia pestis* Caused the Black Death. *PLoS Pathog* 6(10): e1001134. doi:10.1371/journal.ppat.1001134

Editor: Nora J. Besansky, University of Notre Dame, United States of America

Received: May 20, 2010; **Accepted:** September 7, 2010; **Published:** October 7, 2010

Copyright: © 2010 Haensch et al. This is an open-access article distributed under the terms of the Creative Commons Attribution License, which permits unrestricted use, distribution, and reproduction in any medium, provided the original author and source are credited.

Funding: This research was supported by grants from the Deutsche Forschungsgemeinschaft (DFG Br 2065/1-1 and Br 2995/1-2), the University of Mainz (FP1-2007) and the Science Foundation of Ireland (0501E1882). The aDNA analysis was supported by Compagnia di San Paolo (2007-0173). The funders had no role in study design, data collection and analysis, decision to publish, or preparation of the manuscript.

Competing Interests: The authors have declared that no competing interests exist.

* E-mail: bramanti@uni-mainz.de

Introduction

Of the numerous epidemics in human history, three pandemics are generally accepted as having been caused by plague. Justinian's plague (AD 541–542) spread from Egypt to areas surrounding the Mediterranean [1]. In 1347, an epidemic known as the Black Death spread from the Caspian Sea to almost all European countries, causing the death of one third of the European population over the next few years [2]. This second pandemic persisted in Europe until 1730, causing successive and progressively declining epidemic waves. A third plague pandemic began in the Yunnan region of China in the mid-19th century, and spread globally via shipping from Hong Kong in 1854. During this last pandemic, the etiological cause of plague was identified as *Yersinia pestis*, a Gram-negative bacterium [3,4]. Most microbiologists and epidemiologists believe that *Y. pestis* was also the etiological agent of the first two pandemics. This belief is supported by ancient DNA (aDNA) analyses which identified

sequences specific for *Y. pestis* in the teeth of central European plague victims from the first and second pandemics [5–7]. Moreover, the *Y. pestis* F1 protein capsule antigen has been detected in ancient plague skeletons from Germany and France by immunohistochemistry [8].

Based on studies on modern strains, microbiologists have subdivided *Y. pestis* into three biovars: Antiqua, Medievalis, and Orientalis. These biovars can be distinguished depending on their abilities to ferment glycerol and reduce nitrate [10]. The Medievalis biovar is unable to reduce nitrate due to a G to T mutation that results in a stop codon in the *napI* gene [11], while the Orientalis biovar cannot ferment glycerol because of a 93 bp deletion in the *gloD* gene [11,12]. Conversely, the Antiqua biovar is capable of performing both reactions [10]. An apparent historical association of the routes of the three pandemics with the modern geographical sources of the three biovars led DeLignat to propose that each plague pandemic was caused by a different biovar [10]. There is no doubt that the ongoing third pandemic

Yersinia pestis DNA from Skeletal Remains from the 6th Century AD Reveals Insights into Justinianic Plague

Michaela Harbeck¹, Lisa Seifert², Stephanie Hänisch^{3,4}, David M. Wagner⁵, Döner Birdsell⁶, Katy L. Parise⁵, Ingrid Wlechlmann⁶, Gisela Grube^{1,2}, Astrid Thomas⁷, Paul Keim⁸, Lothar Zöllner⁹, Barbara Bramanti^{3,4,9}, Julia M. Riehm⁷, Holger C. Scholtz^{2*}

1 State Collection for Anthropology and Paleontology, Marck, Germany, **2** Department Biology I Anthropology and Human Genetics, Ludwig Maximilian University of Munich, Marquardt, Germany, **3** Institute for Anthropology, Johannes Gutenberg University, Mainz, Germany, **4** Centre for Biological and Forensic Sciences (CEFS), Organization Collaborating, Antananarivo, Madagascar, **5** Department of Anatomy and Embryology, Medical Faculty, Georg-August University, Göttingen, Germany, **6** UMR, Villeveuve d'Asco, Archeological Center, Villeveuve d'Asco, France, **7** UMR, Villeveuve d'Asco, Archeological Center, Villeveuve d'Asco, France, **8** Department of Microbial Genetics and Genomics, Northern Arizona University, Flagstaff, Arizona, United States of America, **9** Institute of Paleontology, Domestication Research and the History of Veterinary Medicine, Department of Veterinary Sciences, Ludwig Maximilian University of Munich, Munich, Germany, **10** Biogen Anthropology, Department of Anatomy and Embryology, Leiden University Medical Center, Leiden, The Netherlands

Abstract

Yersinia pestis, the etiological agent of the disease plague, has been implicated in three historical pandemics. These include the third pandemic of the 19th and 20th centuries, during which plague was spread around the world, and the second pandemic of the 14th–17th centuries, which included the infamous epidemic known as the Black Death. Previous studies have confirmed that *Y. pestis* caused these two more recent pandemics. However, a highly spited debate still continues as to whether *Y. pestis* caused the so-called Justinianic Plague of the 6th–8th centuries AD. By analyzing ancient DNA in two independent ancient DNA laboratories, we confirmed unambiguously the presence of *Y. pestis* DNA in human skeletal remains from an Early Medieval cemetery. In addition, we narrowed the phylogenetic position of the responsible strain down to major branch 0 on the *Y. pestis* phylogeny, specifically between nodes N03 and N05. Our findings confirm that *Y. pestis* was responsible for the Justinianic Plague, which should end the controversy regarding the etiology of this pandemic. The first genotype of a *Y. pestis* strain that caused the Late Antique plague provides important information about the history of the plague bacillus and suggests that the first pandemic also originated in Asia, similar to the other two plague pandemics.

Citation: Harbeck M, Seifert L, Hänisch S, Wagner DM, Birdsell D, et al. (2010) *Yersinia pestis* DNA from Skeletal Remains from the 6th Century AD Reveals Insights into Justinianic Plague. *PLoS Pathog* 6(10): e1001134. doi:10.1371/journal.ppat.1001134

Editor: Nora J. Besansky, University of Notre Dame, United States of America

Received: December 19, 2010; **Accepted:** March 24, 2011; **Published:** May 7, 2011

Copyright: © 2010 Harbeck et al. This is an open-access article distributed under the terms of the Creative Commons Attribution License, which permits unrestricted use, distribution, and reproduction in any medium, provided the original author and source are credited.

Funding: This work was supported by a PhD scholarship from the Austrian graduate school G0 program, the US Department of Homeland Security (2010-ST-09-00015), 04K2K-10-C-00129, and the Deutsche Forschungsgemeinschaft (DFG Br 2065/1-2). The funders had no role in study design, data collection and analysis, decision to publish, or preparation of the manuscript.

Competing Interests: The authors have declared that no competing interests exist.

* E-mail: M.Harbeck@zoo.uni-muenchen.de (MH); holger.scholtz@bundestuehns.de (HCS); bramanti@uni-mainz.de (BB)

Introduction

In 541 AD, eight centuries before the Black Death, a deadly infectious disease hit the Byzantine Empire, reaching Constantinople in 542 and North Africa, Italy, Spain, and the Fränkisch-German border by winter 543 [1]. The so-called "Plague of Justinian", named after the contemporaneous emperor, led to mass mortality in Europe similar to that of the Black Death. It persisted in the territory of the Roman Empire until the middle of the 8th century and likely contributed to its decline, shaping the end of antiquity [1]. Based on historical records, this disease has been diagnosed as bubonic plague although discrepancies between historical sources and the progression of *Y. pestis* infections have led some authors to propose that the Plague of Justinian was caused by a different pathogen (as discussed in [2]). This vaccination discussion was recently reinforced by an ancient DNA study of the second pandemic that also questioned whether *Y. pestis* was truly the causative agent of the first pandemic [3,4].

Western scientists have traditionally subdivided *Y. pestis* strains into three biovars: Antiqua, Medievalis, and Orientalis, depending on their abilities to ferment glycerol and reduce nitrate [5].

However, this system ignores many other *Y. pestis* biovars that have been designated and described by other scientists [see 6,7]. Biovars, which are based upon phenotypic properties, do not always correspond directly to specific molecular groups because the same phenotype can result from different mutations [9]. As a result, it has been suggested that groupings within *Y. pestis*, or assignment of unknown strains to specific populations should be based upon molecular signatures and not phenotypes [9]. Fortunately, the recent construction of highly-accurate rooted global phylogenetic trees for *Y. pestis* [10,11] (reproduced in Figure 1) have facilitated the assignment of isolates to distinct populations. The most recent global phylogeny is based upon single nucleotide polymorphisms (SNPs) identified from the genomes of 135 global strains [11]. All clones that caused the third pandemic belong to populations assigned to the molecular group L.ORI [10,11]; the basal node for this group is N14 (Figure 1).

Two recent studies [3,12] have queried key SNPs in DNA samples obtained from victims of the second pandemic (14th century AD), facilitating the phylogenetic placement of these samples in the most recent global phylogeny [11]. These samples are along the branch between nodes N07 and N10 (Figure 1) close

REPEATED INTRODUCTIONS OF PLAGUE FROM OUTSIDE EUROPE

Yersinia pestis

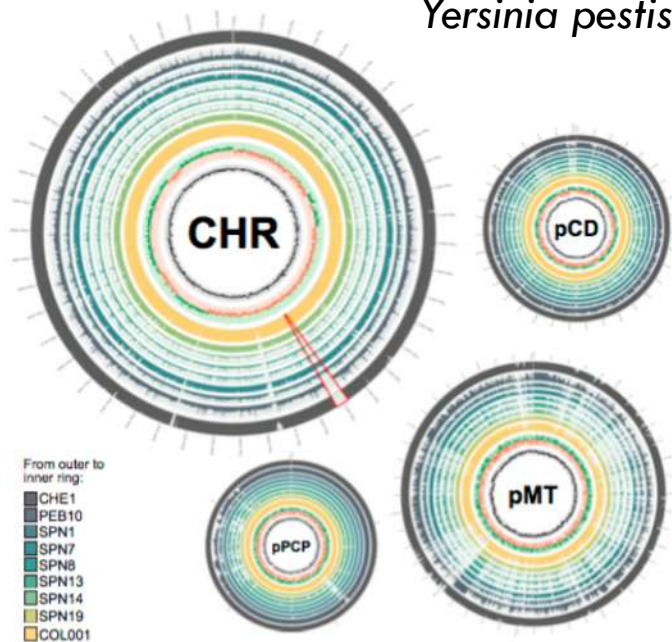


Fig. 1. Coverage plots for nine genomes to *Y. pestis* CO92. Plots represent the chromosome and each of the three CO92 plasmids (CHR: chromosome). Rings (from outer to inner ring) show coverage rings 1 to 95. GC skew ring 105, and GC content ring 111, range: 30 to 3076. aDNA genomes are ordered as follows (from outer to inner ring): CHE1, PEB10, SPN1, SPN7, SPN8, SPN13, SPN14, SPN19, and COL001. Coverage cutoff for PEB10, CHE1, and COL001 is 15x and 6x for all SPN samples. Plots were created with Circos (23). The chromosomal plots were calculated in 2,000-bp windows, the plots for pMT and pPCP in 50-bp windows, and the plot for pCD in 10-bp windows. The 49-kbp deletion is marked in red on the chromosomal plot.



Fig. 2. Historically reconstructed introduction routes of *Y. pestis* for available 18th century genomes, consisting of multiple spatiotemporal waves. Locations shown and highlighted on the map are discussed in this study. Sites for which genomic data were published in previous studies are marked with an asterisk. Basemap is from Wikimedia.